PL-TR-92-2252

THEORETICAL AND EXPERIMENTAL RESEARCH IN INFRARED TECHNOLOGY

Chun C. Lin

University of Wisconsin-Madison
Department of Physics
Madison, Wisconsin 53706

31 December 1992

Final Report
26 March 1986-30 September 1992

PHILLIPS LABORATORY
Directorate of Geophysics
AIR FORCE MATERIEL COMMAND
HANSCOM AIRFORCE BASE, MA 01731-5000

"This technical report has been reviewed and is approved for publication"

EDWARD T.P. LEE
Contract Manager

WILLIAM A.M. BLUMBERG
Branch Chief

ROGER A. VANTASSEL
Division Director

This report has been reviewed by the ESC Public Affairs Office (PA) and is releasable to the National Technical Information Service (NTIS).

Qualified requestors may obtain additional copies f rom the Defense Technical Information Center. All others should apply to the National Technical Information Service.

If your address has changed, or if you wish to be removed from the mailing list, or if the addressee is no longer employed by your organization, please notify PL/TSI, Hanscom AFB, MA 01731-5000. This will assist us in maintaining a current mailing list.

Do not return copies of this report unless contractual obligations or notices on a specific document requires that it be returned.

REPORT DOCUMENTATION PAGE

Form Approved
OMB No 0704 0188

1. AGENCY USE ONLY (Leave blank)	2. REPORT DATE	3. REPORT TYPE AND DATES COVERED
	31 December 1992	Final (26 March 1986-30 Sep 1992)

4. TITLE AND SUBTITLE
Theoretical and Experimental Research in Infrared Technology

5. FUNDING NUMBERS
PE 61102F
PR 2310 TA G4 WU BP

Contract F19628-86-C-0076

6. AUTHOR(S)
Chun C. Lin

7. PERFORMING ORGANIZATION NAME(S) AND ADDRESS(ES)
University of Wisconsin-Madison
Department of Physics
Madison, Wisconsin 53706

8. PERFORMING ORGANIZATION REPORT NUMBER

9. SPONSORING/MONITORING AGENCY NAME(S) AND ADDRESS(ES)
Phillips Laboratory
Hanscom AFB, MA 01731-5000

Contract Manager: Edward T.P. Lee/GPOS

10. SPONSORING/MONITORING AGENCY REPORT NUMBER
PL-TR-92-2252

11. SUPPLEMENTARY NOTES

12a. DISTRIBUTION/AVAILABILITY STATEMENT
Approved for public release;
Distribution unlimited

12b. DISTRIBUTION CODE

13. ABSTRACT *(Maximum 200 words)*
This report includes research on (a) electron-impact ionization of oxygen atoms (b) rate constants for three-body recombination of electrons with atomic oxygen ions (c) electronic structure of Rydberg oxygen molecules (d) electron-impact excitation of Rydberg oxygen molecules (e) electron-impact emission cross sections of the oxygen Second Negative Bands (f) formation of highly excited states by electron recombination with atomic and molecular oxygen ions.

14. SUBJECT TERMS		15. NUMBER OF PAGES
Rydberg oxygen atoms	Three-body recombination	58
Rydberg oxygen molecules	Electron-impact excitation	16. PRICE CODE
Electron-impact ionization	Oxygen second negative bands	
	Radiative recombination	

17. SECURITY CLASSIFICATION OF REPORT	18. SECURITY CLASSIFICATION OF THIS PAGE	19. SECURITY CLASSIFICATION OF ABSTRACT	20. LIMITATION OF ABSTRACT
Unclassified	Unclassified	Unclassified	SAR

TABLE OF CONTENTS

PART 1

PART 2

PART 3

PART 4

PART 5

PART 6

PART 1

ELECTRON-IMPACT IONIZATION OF THE OXYGEN ATOM

1. INTRODUCTION

Electron-impact ionization of the oxygen atom is an important basic process in atmospheric and plasma physics. Experimental measurements of ionization of atoms and molecules including oxygen atom have been reviewed by Kieffer and Dunn [1]. More recent complications of ionization data are given by Laher and Gilmore [2], and by Bell et al. [3]. The electron-impact ionization cross sections of the oxygen atom were measured by Fite and Brackmann [4], Rothe et al. [5], Brook et al., [6] and Zipf [7]. In the first two experiments [4,5] a partially dissociated oxygen beam containing O_2 and O was used to measure the ratio of the ionization cross sections of the two species, $\sigma(O^+)/\sigma(O_2{}^+)$, which, upon combining with the total molecular ionization cross sections of Tate and Smith [8], gives $\sigma(O^+)$. Brook et al. [6] used the charge-exchange process as the source of atomic oxygen beam. Zipf [7] used a beam of O/O_2 mixture, but the normalization procedure was different. Zipf [7] also revised the data of Fite and Brackmann [4] using the newer O_2 ionization cross sections of Mark [9].

An early calculation of ionization cross sections of oxygen atoms [10] was made by utilizing the relationship between the electron-impact and photoionizaton cross sections. Subsequent calculations [11-16] involve the Born approximation, and in all but one case [16] the hydrogenic Coulomb functions were used to describe the ionized electrons and the 2p atomic wave functions were obtained by various means. The Coulomb functions were orthogonalized to the 2p function by the customary (but somewhat arbitrary) procedure. Peach [11] used the 2p function of Clementi [17], and computed the cross sections with both the Born and Born-Ochkur approximations. Other kinds of 2p atomic wave functions were used in Refs. 13-15 as explained in the respective papers. Burnett and Rountree [16] computed the ionization cross sections by the Born approximation with no allowance for the electron exchange, but with

a set of wave functions much more elaborate than the ones used in other works [11-15]. For the initial state of the target atom, a six-term configuration interaction (CI) wave function is used to describe the ground state of the oxygen atom O(^{3}P). The continuum wave functions for the ejected electron in the final target state are determined by solving the close-coupling equations that result from the inclusion of the ^{4}S, ^{2}D, and ^{2}P terms of the $2p^3$ configuration of the free O^+ ion in the Schroedinger equation for the target.

In this paper we conduct a systematic theoretical study for the electron-impact ionization of the oxygen atom from the excited states as well as from the ground state. We start with the Born approximation to calculate the ionization cross section of the ground-state O(^{3}P) oxygen atoms, and treat the electron exchange using the procedure suggested by Ochkur [18], i.e., the Born-Ochkur approximation. To improve the cross sections at low energies, we replace the Born-type approximation by the method of (exchange) distorted waves with Ochkur's exchange. The calculation is extended to some low-lying excited oxygen atoms in the $2p^3(^4S)n_o\ell_o\ ^3L_o$ states. To calculate the wave functions, we use the frozen-core approximation by which we assume that 1s, 2s, 2p functions remain unchanged in the O(^{3}P), O[(^{4}S)$n_o\ell_o\ ^3L_o$], and O^+(^{4}S,^{2}D,^{2}P) states. The wave functions of the excited orbitals $n_o\ell_o$, of the ejected electron, and of the distorted projectile electron are computed by the Hartree-Fock procedure while those of 1s, 2s, 2p, are taken from the paper of Clementi and Roetti [19].

In Section 2 we set the theoretical framework under which the cross sections are calculated. In Section 3 we present the results and compare them with the previous theoretical calculations and with the experimental measurements. Section 4 concludes the paper.

2. THEORY

A. General Description and the Born-Ochkur Approximation

Since the theory of electron-impact ionization of atoms has been treated extensively by Peterkop [20], Rudge and Seaton [21], and Rudge [22], we will cite the relevant results developed in those papers without detailed explanations. Let us first consider the simplest

case of e-H ionizing collision where an incident electron of momentum $\hbar\vec{k}_o$ impinges on the hydrogen atom of wave function $\phi_o(\vec{r}_2)$ resulting in a scattered electron of momentum $\hbar\vec{k}_1$ and an ionized electron of momentum $\hbar\vec{k}_2$. The kinetic energies of the electrons are related as

$$k_o^2 - 2I = k_1^2 + k_2^2, \tag{1}$$

where I is the ionization potential energy in au. The bound-state function $\phi_o(\vec{r})$ is expresed as

$$\phi_o(\vec{r}) = R_{n_o l_o}(r) Y_{l_o m_o}(\hat{r}) = r^{-1} P_{n_o l_o}(r) Y_{l_o m_o}(\hat{r}), \tag{2}$$

and the wave function of the ionized electron $\phi(\vec{k}_2,\vec{r})$ as

$$\phi(\vec{k}_2,\vec{r}) = \Sigma_{l=0}^{\infty} \Sigma'_{m=-l} R_{\epsilon l}(r)\ Y_{lm}(\hat{r}) Y_{lm}(\hat{k}_2). \tag{3}$$

Here we used symbol ϵ, which is $k_2^2/2$, to indicate the energy of the ionized electron. As indicated in Eq. (2) we use $P_{nl}(r)$ to designate the "reduced" radial wave function $rR_{nl}(r)$. The cross sections of this process are dictated by the direct and exchange amplitudes, $f(\vec{k}_1,\vec{k}_2)$ and $g(\vec{k}_1,\vec{k}_2)$. Discussions of f and g can be found in, for example, the paper by Rudge and Seaton [21] where the symbols $\vec{k}$ and $\vec{k}'$ are used in place of our $\vec{k}_1$ and $\vec{k}_2$. The ionization cross section integrated over all directions of $\vec{k}_1$ and $\vec{k}_2$ is given by

$$\left(\frac{d\sigma}{d\varepsilon}\right)^{\pm} = (k_1 k_2/k_o) \int |f(\vec{k}_1,\vec{k}_2) \pm g\ (\vec{k}_1,\vec{k}_2)|^2 d\hat{k}_1 d\hat{k}_2, \tag{4}$$

where the superscripts "+" and "–" on the left-hand side correspond to scattering states with total spin 0 and 1 respectively. If the H atom is ionized by unpolarized electrons, then the cross section is the weighted average of the "+" and "–" with the statistical weight 1:3.

In the Born approximation (with no exchange), the g term is neglected and the f term is approximated by

$$f(\vec{k}_1\vec{k}_2) \simeq -(1/2\pi) \int e^{i\vec{k}_o\cdot\vec{r}_1}\ \ \phi_o(\vec{r}_2)\ \ |\vec{r}_1 - \vec{r}_2|^{-1}\ e^{-i\vec{k}_1\cdot\vec{r}_1}\ \phi^*(\vec{k}_2,\vec{r}_2)\ d\vec{r}_1 d\vec{r}_2, \tag{5}$$

where $\phi_o(\vec{r}_2)$ and $\phi(\vec{k}_2,\vec{r}_2)$ are defined in Eqs.(2) and (3). Alternatively, one can adopt the Born-Oppenheimer approximation in which g is taken from Eq.(5) by permuting the two electrons in the final state, i.e.,

$$g(\vec{k}_1,\vec{k}_2) = -(1/2\pi)\int e^{i\vec{k}_o\cdot\vec{r}_1}\ \phi_o(\vec{r}_2)|\vec{r}_1-\vec{r}_2|^{-1}\ e^{-i\vec{k}_1\cdot\vec{r}_2}\ \phi^*(\vec{k}_2,\vec{r}_1)\ d\vec{r}_1 d\vec{r}_2. \tag{6}$$

The use of the Born-Oppenheimer exchange amplitude of Eq.(6) leads to the well known difficulty of overestimating the cross sections especially at incident energies near the threshold. Ochkur [18] has suggested an approximation for treating the exchange amplitude for ionization processes, i.e.,

$$g(\vec{k}_1,\vec{k}_2) \simeq f(\vec{k}_1,\vec{k}_2)|\vec{k}_o-\vec{k}_1|^2/\ (k_o^2-k_2^2). \tag{7}$$

This Born-Ochkur (BO) approximation is shown to yield much closer agreement with experiment for e-H ionization than the Born approximation or the Born-Oppenheimer approximation [18]. In the present work we shall use Eq.(7) to compute exchange amplitude yielding

$$\left(\frac{d\sigma}{d\varepsilon}\right)^{\pm}_{BO} = (k_1k_2/k_o)\int (X^{\pm})^2|f(\vec{k}_1\vec{k}_2)|^2 d\hat{k}_1 d\hat{k}_2, \tag{8}$$

with

$$X^{\pm} = 1 \pm |\vec{k}_o-\vec{k}_1|^2/(k_o^2-k_2^2). \tag{9}$$

Following Peterkop [20] we evaluate Eq.(8) by re-expressing f($\vec{k}_1$,$\vec{k}_2$) of Eq.(5) as

$$f(\vec{k}_1,\vec{k}_2) = -2K^{-2} < 0|\vec{K}|\vec{k}_o>, \tag{10}$$

$$\vec{K} = \vec{k}_o-\vec{k}_1, \tag{11}$$

$$< 0|\vec{K}|\vec{k}_2 > = \int \phi_o(\vec{r}_2)e^{i\vec{K}\cdot\vec{r}_2}\ \phi^*(\vec{k}_2,\vec{r}_2)d\vec{r}_2. \tag{12}$$

Integration over $d\hat{k}_1$ and $d\hat{k}_2$ reduces Eq. (8) to

$$\left(\frac{d\sigma}{d\varepsilon}\right)^{\pm}_{BO} = 8\pi k_o^{-2}\int_{K_{min}}^{K_{max}} (X^{\pm})^2|\ < n_o l_o\ |K|\varepsilon >\ |^2 K^{-3}dK, \tag{13}$$

$$| < n_o l_o | K | \varepsilon > |^2 = (2l_o + 1)^{-1} \Sigma_{m_o l m} | \int R_{n_o l_o}(r) Y_{l_o}(\hat{r}) e^{i\vec{K}\cdot\vec{r}} R_{\varepsilon l}(r) Y^*_{lm}(\hat{r}) d\vec{r}|^2. \quad (14)$$

The integration limits K_{min} and K_{max} in Eq. (13) are the (absolute value of) difference and sum of k_o and k_1 respectively. The cross sections are averaged over the initial magnetic substrates m_o as indicated in Eq. (14). The total ionization cross section is

$$\sigma^{\pm}(E) = \int_o^{E_{max}/2} \left(\frac{d\sigma}{d\varepsilon}\right)^{\pm} d\varepsilon, \quad (15)$$

where E is the incident-electron energy and

$$E_{max} = E - |I| - k_1^2/2. \quad (16)$$

The upper limit in Eq. (15) is set to $E_{max}/2$ instead of E_{max}, since a close examination [20-22] shows that $g(\vec{k}_2,\vec{k}_1)$ and $f(\vec{k}_1,\vec{k}_2)$ describe the same physical occurrence. To avoid this redundancy, the upper limit in Eq. (15) is set to $E_{max}/2$.

Comparison of the BO cross sections for ionization of the H atom with those obtained by the Born approximation shows that inclusion of exchange does not greatly alter the cross sections except at low energies. For example, by reading the figure in Ref. 18, we see that the ratios of the BO cross sections to the Born cross sections are about 0.65, 0.75, 0.83, and 0.89 at 25, 50, 100, and 200 eV respectively.

B. Method of Distorted Waves

In the Born approximation, plane waves $e^{i\vec{k}_o\cdot\vec{r}}$ and $e^{i\vec{k}_1\cdot\vec{r}}$ are used for the incident and scattered waves. Because of the interaction of the projectile electron with the target atomic electrons and nucleus, departure from plane wave is expected. The method of distorted wave (DW) attempts to correct for this departure, and has been applied to electron-impact excitations and ionization of atoms [23-25]. To simplify the formulation we may, without loss of generality, assume the direction of the incident electron to be the z-direction. With allowance for distortion by the target, the incident-electron function is expanded as

$$\phi(\vec{k}_o,\vec{r}) = (4\pi)^{1/2} \Sigma_{l_1} i^{l_1} (2l_1 + 1)^{1/2} r^{-1} \mathcal{P}_{k_o l_1}(r) Y_{l_1 0}(\hat{r}), \quad (17)$$

while the scattered-wave function is expanded as

$$\phi(\vec{k}_1,\vec{r}) = 4\pi\ \Sigma_{l_2m_2} i^{l_2} r^{-1}\mathcal{P}_{k_1l_2}(r)Y_{l_2m_2}(\hat{r})Y^*_{l_2m_2}(\hat{k}_1) \tag{18}$$

where $r^{-1}\mathcal{P}_{kl}(r)$ denotes the distorted partial waves which are the solutions of the Schroedinger equation for the incident (or scattered) electron in the field of the hydrogen atom. The precise form of the differential equation for the distorted partial waves will be given in Section 2C when we discuss the electron-impact ionization of the oxygen atom [Eq.(42)]. To obtain the DW scattering amplitude we substitute Eqs.(17) and (18) for $e^{i\vec{k}_o\cdot\vec{r}_1}$ and $e^{i\vec{k}_1\cdot\vec{r}_1}$ respectively in Eq. (5), along with

$$\frac{1}{|\vec{r}_1-\vec{r}_2|} = \frac{1}{r_>}\Sigma_{\lambda\mu}\left(\frac{4\pi}{2\lambda+1}\right)\ \left(\frac{r_<}{r_>}\right)^{\lambda} Y^*_{\lambda\mu}(\hat{r}_1)Y_{\lambda\mu}(\hat{r}_2). \tag{19}$$

The DW direct amplitude becomes

$$\begin{aligned} f(\vec{k}_1,\vec{k}_2) &= -4\sqrt{\pi}\Sigma_{l_1l_2m_2} i^{l_1-l_2}(2l_1+1)^{1/2} \\ &\times\ \Sigma_\lambda c^\lambda(l_10,l_2m_2)c^\lambda(lm,l_om_o)\ Y^*_{lm}(\hat{k}_2)Y^*_{l_2m_2}(\hat{k}_1) \\ &\times\ R^\lambda(k_ol_1,n_ol_o,k_1l_2,nl), \end{aligned} \tag{20}$$

where, as defined by Condon and Shortley [26],

$$c^\lambda(l_1m_1,l_2m_2) = [4\pi/(2\lambda+1)]^{1/2}\int Y^*_{l_1m_1}(\hat{r})\ Y_{\lambda,m_1-m_2}(\hat{r})Y_{l_2m_2}(\hat{r})d\hat{r}, \tag{21}$$

and

$$\begin{aligned} R^\lambda(k_ol_1,n_ol_o,k_1l_2,nl) &= \int_o^\infty \mathcal{P}_{k_ol_1}(r)\ \ \mathcal{P}_{k_1l_2}(r)dr \\ \times\left[r^{-\lambda-1}\int_o^r P_{n_ol_o}(x)P_{nl}(x)x^\lambda dx + r^\lambda\int_r^\infty\ P_{n_ol_o}(x)P_{nl}(x)x^{-\lambda-1}dx\right]. \end{aligned} \tag{22}$$

Upon averaging over the initial m_o sublevels and integrating over the directions of the scattered electron and the ejected electron, we have the DW cross sections (neglecting exchange) as

$$\begin{aligned} \left(\frac{d\sigma}{d\varepsilon}\right)_{DW} &= k_1k_2[(2l_o+1)k_o]^{-1}\Sigma_{m_o}\int|f(\vec{k}_1,\ \vec{k}_2)|^2d\hat{k}_1d\hat{k}_2 \\ &= 16\pi k_1k_2[(2l_o+1)k_o]^{-1}\Sigma_{lml_1l_2m_2}(2l_1+1) \\ &\times\ \Sigma_\lambda[c^\lambda(l_10,l_2m_2)c^\lambda(lm,l_om_o=m-m_2) \\ &\times\ R^\lambda(k_ol_1,n_ol_o,k_1l_2,nl)]^2. \end{aligned} \tag{23}$$

The exchange amplitude can be obtained from Eq.(6) by the similar substitutions for the incident and scattered waves. However, such an analog of the Born-Oppenheimer exchange amplitude leads to unreasonably large cross sections. Therefore, we shall again resort to Ochkur's results [18], and assume that f and g are related by Eq.(7). However, since Eq. (7) was based on the plane-wave approximation, the use of this equation to determine g from f in a DW-type calculation must be viewed as a further step of approximation. Nevertheless the contribution to the ionization cross sections from g is usually much smaller than from f. Thus a DW calculation along with an Ochkur-like exchange should be a significant improvement over the Born-Oppenheimer approximation for ionization calculations. Following Eq. (7), we write

$$\begin{aligned} g/f &= |\vec{k}_o - \vec{k}_1|^2 / \left(k_o^2 - k_2^2\right) \\ &= \left(k_o^2 + k_1^2 - 2k_o k_1 cos\theta_1\right) / \left(k_o^2 - k_2^2\right) \\ &= (a - b cos\theta_1)\,, \end{aligned} \tag{24}$$

where a and b are $(k_o^2 + k_1^2)/(k_o^2 - k_2^2)$ and $2k_o k_1/(k_o^2 - k_2^2)$ respectively, and θ_1 is the angle $\hat{k}_1$ makes with z-axis ($\hat{k}_o$ being in the z-direction).

Corresponding to the plane-wave Born-Ochkur cross section $\left(\frac{d\sigma}{d\varepsilon}\right)^+_{BO}$, we express the cross sections based on the exchange distorted wave method with the Ochkur approximation (EDWO) as

$$\begin{aligned} \left(\frac{d\sigma}{d\varepsilon}\right)^+_{EDWO} &= k_1 k_2 \left[(2l_o + 1)\, k_o\right]^{-1} \Sigma_{m_o} \int |f + f\,(a - b cos\theta_1)\,|^2 d\hat{k}_1 d\hat{k}_2 \\ &= I_0 + I_1 + I_2, \end{aligned} \tag{25}$$

where I_0 is $[(a+1)^2+b^3/3]$ times the $(d\sigma/d\varepsilon)_{DW}$ of Eq. (23), and

$$\begin{aligned} I_j &= \alpha_j \, \Sigma_{lm\lambda \, l_1 l_2 m_2 l_1' l_2'} i^{(l_1 - l_2 - l_1' + l_2')} \\ &\times \; c^\lambda (l_1 0, l_2 m_2)\, c^\lambda (lm, l_o m_o = m - m_2) \\ &\times \; R^\lambda (k_o l_1, n_o l_o, k_1 l_2, nl) \end{aligned}$$

$$\times \quad c^{\lambda}\left(l_1'0, l_2'm_2\right) c^{\lambda}\left(lm, l_o m_o = m - m_2\right)$$

$$\times \quad R^{\lambda}\left(k_o l_1', n_o l_o, k_1 l_2', nl\right)$$

$$\times \quad c^{j}\left(l_2 m_2, l_2' m_2\right), \; j = 1, 2 \tag{26}$$

with

$$\alpha_1 \;=\; -2b(a+1), \tag{27}$$

$$\alpha_2 \;=\; 2b^2/3. \tag{28}$$

Equations (25) and (26) represent an exact transcription of Ochkur's formula to the DW calculation of ionization. However, a much simpler expression is obtained in Eq.(24) if we make use of the fact that for excitation to an optically allowed state as well as ionization, the scattering is strongly peaked in the forward direction. Thus we replace $\mid \vec{k}_o\text{-}\vec{k}_1 \mid^2$ by $(k_o - k_1)^2$ in Eq.(24), so that

$$g \;=\; f\gamma, \tag{29}$$

$$\gamma \;=\; (k_o - k_1)^2 \,/\, \left(k_o^2 - k_2^2\right), \tag{30}$$

and

$$\left(\frac{d\sigma}{d\varepsilon}\right)^{+}_{EDWO} = k_1 k_2 [(2l_o + 1)\, k_o]^{-1} (1+\gamma)^2 \, \Sigma_{m_o} \int |f\left(\vec{k}_1, \vec{k}_2\right)|^2 d\hat{k}_1 d\hat{k}_2. \tag{31}$$

We have made some test calculations using as example the bound-state excitations from $O(3p^4\ ^3P)$ to $O[2p^3(^4S)3s\ ^3S]$ and to $O[2p^3(^4S)3d\ ^3D]$. The use of Eq.(31) gives cross sections that are larger than the ones from Eqs.(25) and (26) by about 10% near the threshold. Beyond the threshold, the difference quickly decreases to the 3-5% range with increasing incident energy. In view of such small differences, we use this simplified version of Ochkur's approximation in our calculations.

C. Ionization of Oxygen Atoms

In this paper we consider the ionization processes:

$$e^- \;+\; O\left(2p^4\ ^3P\right) \rightarrow e^- + e^- + O^+\left(2p^3\ ^4S,\ ^2D,\ ^2P\right), \tag{32}$$

$$e^- \;+\; O[\left(2p^3\ ^4S\right) n_o l_o\ ^3L_o] \rightarrow e^- + e^- + O^+\left(2p^3\ ^4S\right). \tag{33}$$

We first determine the relevant orbitals of the oxygen atom (in the absence of the colliding electron) corresponding to the $O(2p^4\ ^3P)$ and $O[(2p^3\ ^4S)\ n_o\ell_o\ ^3L_o]$ bound states and the $[O^+(2p^3\ ^4S,^2D,^2P) + e^-]$ continuum states by the Hartree-Fock method with a frozen-core approximation in which the 1s,2s,2p orbitals are treated as fixed and identical to the corresponding orbitals for the $(2p^4)^3P$ state of the oxygen atom as given by Clementi and Roetti [19]. Detailed procedures for calculting the $n_o\ell_o$-orbitals and the continuum-state orbitals have been described previously [27,28]. Analogous to the notation in Section 2A, we use $\phi_o(\vec{r})$ for the active electron (2p or $n_o\ell_o$) of the initial target state, and $\phi_f(\vec{k}_2,\vec{r})$ for the ejected electron. The latter is a superposition of angular momentum states of different ℓ,m values and behave at large distance like a particle of momentum $\hbar\vec{k}$ as indicated in Ref. 28. It is worth noting that the orthogonality condition is incorporated into the differential equation for the continuum-state orbitals [28], thereby obviating the arbitrary orthogonalization procedure at a later stage of the calculation.

Ionization is produced by the interaction of the colliding electron with the O atom

$$H_{int} = -\frac{Z}{r_1} + \Sigma_{j=2}^{9}|\vec{r}_1 - \vec{r}_j|^{-1}, \tag{34}$$

where the nuclear charge Z is 8, and we labeled the colliding electron as 1. Since H_{int} is independent of spin, we construct the spin eigenfunctions of the colliding system. For example, in the case of Eq. (32) we have for the initial state

$$\begin{aligned}\Psi_o(S,M|\vec{x}_1,\vec{x}_2,...\vec{x}_9) \;&=\; \mathcal{A}\Sigma_\mu C\,(1/2,\ \mu,\ 1,\ M-\mu;\ SM)\\ &\qquad \phi_c\,(1/2,\ \mu|\vec{x}_1)\,\Phi_o\,(1,M-\mu|\vec{x}_2,...,\vec{x}_9)\,,\end{aligned} \tag{35}$$

where $C(j_1, m_1, j_2, m_2; jm)$ is the Clebsch-Gordan coefficient, Φ_o denotes the wave functions of the oxygen atom in the $(2p^4)^3P$ state, and the colliding electron is represented by ϕ_c which will be described later. We use $\vec{x}_i$ to represent the spatial-spin coordinates, and $\mathcal{A}$ for the antisymmetrization operator. To construct the final-state wave function for Eq.(32), we first

couple the O^+-ion function (Φ^+) with the spin-orbital of the ejected electron (ϕ_{ej}) to form the intermediate states, Φ_{in}, i.e.,

$$\Phi_{in}(S_1M_1|\vec{x}_2,...,\vec{x}_9) = \mathcal{A}\Sigma_\mu C(1/2,\ \mu,\ 1,\ M_1-\mu;\ S_1M_1) \phi_{ej}\left(1/2,\ \mu,\vec{k}_2|\vec{x}_2\right)\Phi^+(3/2,\ M_1-\mu|\vec{x}_3,...,\vec{x}_9), \quad (36)$$

which are then coupled with the colliding electron function ϕ_c to form $\Psi_f(S'M' \mid x_1,....x_9)$. The scattering amplitudes are obtained by

$$\mathcal{F}^S = (1/2\pi)\int \Psi_f^*(SM|\vec{x}_1,...,\vec{x}_9)\, H_{int}\Psi_o(SM|\ \vec{x}_1,...,\vec{x}_9)\, d\vec{x}_1...d\vec{x}_9, \quad (37)$$

which are diagonal in (SM) and independent of M. As a consequence of Ψ_o and Ψ_f being antisymmetrized, $\mathcal{F}^S$ includes both the direct f and exchange g amplitudes.

Next we sum the cross sections over S and M, and divide by $2(2S_1+1)$, the number of the possible initial spin states, S_1 being the spin of the initial atomic state, so that the results correspond to ionization by a beam of unpolarized electrons. By a straight-forward calculation, we find

$$\frac{d\sigma}{d\varepsilon} = (k_1k_2/k_o)\,\Sigma_S[(2S+1)/2(2S_1+1)]\int|\mathcal{F}^S|^2 d\hat{k}_1 d\hat{k}_2 \quad (38)$$

$$= (k_1k_2/k_o)\int\left(|f|^2 - fg + |g|^2\right)d\hat{k}_1 d\hat{k}_2, \quad (39)$$

$$f = -2K^{-2}C_{FP}\int\phi_o(\vec{r})\,e^{i\vec{K}\cdot\vec{r}}\phi_f^*\left(\vec{k}_2,\ \vec{r}\right)d\vec{r}, \quad (40)$$

where C_{FP} stands for the coefficients of fractional parentage that arise due to the equivalent 2p orbitals in process (32), and is numerically equal to $\sqrt{4/3}$, $\sqrt{5/3}$,and 1 respectively for the ^4S, ^2D and ^2P final states of O^+[29]. For process (33) the issue of fractional parentage does not arise, i.e., C_{FP}=1. The g amplitude is related to f through Eq.(7) or Eq.(29). Notice that there are no superscipts on the left-hand side of Eq.(38), since the cross section corresponds to ionization by unpolarized electrons.

To calculate the BO cross sections, $\phi_c(\vec{r})$ is taken as the incident plane wave $\exp(i\vec{k}_o\cdot\vec{r})$ in Ψ_o and as $\exp(i\vec{k}_1\cdot\vec{r})$ in Ψ_f, and Eq.(7) is used to express g in terms of f. This gives

$$\left(\frac{d\sigma}{d\varepsilon}\right)_{BO} = \left(8\pi/k_o^2\right) C_{FP}^2 \int_{K_{min}}^{K_{max}} \left(k_o^2 - k_2^2\right)^{-2} \left[\left(k_o^2 - k_2^2\right)^2 - K^2\left(k_o^2 - k_2^2\right) + K^4\right] \times \; | < n_o l_o | K | \varepsilon > |^2 K^{-3} dK. \tag{41}$$

For the EDWO calculations, ϕ_c takes on the more complicated form as given by Eqs.(17) and (18). In these equations the distorted partial waves are the solution of

$$\left[\frac{d^2}{dr^2} - \frac{l(l+1)}{r^2} - V(r) + k^2\right] \mathcal{P}_{kl}(r) = \Sigma_{n'l'} W_{n'l',kl}(r)\, P_{n'l'}(r) + \Sigma_{n''} c_{n''l} P_{n''l}(r), \tag{42}$$

where the direct potential V(r) is due to all eight atomic electrons in the oxygen atom for the appropriate initial state in process (32) or (33). Similarly, $W_{n'l',kl}P_{n'l}$ represents the exchange interaction with all the target electrons. The last term in Eq.(42) is to ensure that $\mathcal{P}$ is orthogonal to all the bound $n\ell$ orbitals via the Lagrange multiplier $c_{n''l}$. The details are further described in Ref. 28. The distorted-wave functions of the projectile electron have the asymtotic form (as $r \to \infty$)of

$$\mathcal{P}_{kl}(r) \sim k^{-1} sin\left(kr - \frac{1}{2}l\pi + \zeta_l\right), \tag{43}$$

where ζ_l is the phase shift due to the potentials. As explained earlier, for the distorted-wave calcultion we use the simplified version of the Ochkur exchange as given in Eq.(29). The EDWO cross sections then become

$$\left(\frac{d\sigma}{d\varepsilon}\right)_{EDWO} = 16\pi k_1 k_2 C_{FP}^2 [k_o(2l_o+1)]^{-1} \Sigma_{lml_1l_2m_2}(2l_1+1)\left[1 - \gamma + \gamma^2\right] \times \; \Sigma_\lambda [c^\lambda(l_1 0, l_2 m_2)\, c^\lambda(lm, l_o m_o = m - m_2) \times \; R^\lambda(k_o l_1, n_o l_o, k_1 l_2, nl)]^2, \tag{44}$$

where γ is defined in Eq.(30). The total cross sections σ_{BO} and σ_{EDWO} are then obtained by integrating over ε as indicated in Eq. (15).

3. RESULTS

In order to check the numerical procedures we have computed the ionization cross sections of H(2s) using the numerically tabulated functions for both the bound 2s state and the continuum (Coulomb) functions. In this test calculation we included the angular momenta of the ejected electron $\ell = 0$ - 8. We were able to reproduce the cross sections computed by Prasad [30] within 4% for incident-electron energy from threshold to 200 eV.

In general a greater number of angular momenta ℓ of the ejected electron are needed to achieve convergence as the incident-electron energy is increased. Also, the higher the quantum state from which ionization takes place, the more ℓ's are needed. In this paper we used $\ell = 0$ to $\ell = 30$ in the BO calculations for ionization of the oxygen atoms in the ground state and excited states $(n_o\ell_o)$ up to $n_o = 6$, and used $\ell = 0$ to $\ell = 10$ for the EDWO calculations which cover the ground state and excited states with $n_o = 3$.

The integration with respect to K in Eq. (13) is carried out numerically. The smallest step size ΔK is 4×10^{-4}, and the step size is doubled after 10 quadrature points, except for the eleventh (last) region in which there are 30 points, for a total of 130 points. The rather small ΔK in the beginning is to take care of the steeply rising differential cross sections in the forward direction (i.e., toward small K) of the dipole-allowed transitions, to which all ionization processes belong. Similarly, with regard to ϵ-integration in Eq. (15), we used the initial $\Delta\epsilon = 7.8125 \times 10^{-4}$ a.u., and doubled it after each region. There are eight regions with 10, 10, 10, 10, 40, 20, 20, and 80 quadrature points each.

A. Ionization of $O(2p^4\ ^3P)$ to Form $O^+(2p^3\ ^4S, ^2D, ^2P)$

We have computed the Born (B) and BO cross sections, in the range of 17.5 - 500 eV of the incident electron energy, of ionizing the ground state $O(2p^4\ ^3P)$ atoms and leaving the $O^+(2p^3)$ ions in the three states, ^4S, ^2D, and ^2P. The sum of these three cross sections, which corresponds to ionization of the ground-state oxygen atoms to form $O^+(2p^3)$ ions, is shown in Table 1. We have also applied the EDWO method as well as the method of distorted waves without exchange (DW) to calculate the cross sections at incident energies 17.5 - 200

eV and the results are included in Table 1. Comparison of the B with BO cross sections and of the DW with EDWO cross sections shows that the effect of electron exchange is to reduce the cross sections. At 25 eV this reduction amounts to 11% for B and 18% for DW, whereas at 200 eV, the BO is only 5% below the B cross section, and the difference between EDWO and DW is even smaller. Comparison of the BO and EDWO columns in Table 1 underscores the importance of the distortion of the projectile at low energies. The EDWO cross sections are smaller than the BO cross sections at 25 and 50 eV, but the order is reversed at 75-200 eV. Furthermore the EDWO and BO cross sections tend to merge at increasing energies.

The ionization cross sections of $O(^3P)$ atom have been calculated by several investigators. Peach [11,12] computed ionization cross sections resulting in $O^+(^4S, ^2D, ^2P)$ from the ground state. In the work of Peach [11] the function of Ref. 17 was used for the 2p orbital, and undistorted Coulomb functions of unit nuclear charge (hydrogenic Coulomb functions) were used for the ejected electron. The Born and Born-Ochkur methods were used, thus Peach's work is similar to the present one except for the use of the hydrogenic Coulomb functions. Later the author [12] discovered an error. As a result the cross sections [11] are to be reduced by a factor of two. McGuire [13] computed the Born cross sections by using the wave functions based on the Herman-Skillman potential. Omidvar **et al.** [14] used the scaled hydrogenic functions to compute the Born cross sections. Kazaks **et al.** [15] used the potential of the independent-particle model [31] to determine the wave functions from which the Born cross sections were obtained. Burnett and Rountree [16] reported a Born-approximation calculation using a set of very refined target wave functions. The latter four works [13-16] do not include the effect of electron exchange. In Table 2 we compare our results with those of the previous works. The columns labeled as BAR (Burnett and Rountree [16]), OKS (Omidvar **et al.** [14]), and KGG (**Kazaks et al.** [15]) are our best reading of the figures in the respective papers. The column PEA (Peach [11]) shows the interpolation of Table 4 of Ref. 11 divided by 2 as corrected by Ref. 12. Likewise, the column MCG (McGuire [13]) is an interpolation of Table 4 of Ref. 13. The target wave functions used by Burnett and Rountree

TABLE 1. Electron-impact ionization cross sections (in 10^{-16} cm^2) of ground-state oxygen atoms resulting in O^+ ions in the $(2p^3)^4S$, ^2D, and ^2P states calculated in the present work by using the method of exchange distorted waves with Ochkur's approximation (EDWO); by the method of distorted waves with no exchange (DW); by the Born–Ochkur (BO) approximations and by the Born (B) approximation with no exchange.

E(eV)	EDWO	DW	BO	B
25	0.171	0.210	0.326	0.367
50	0.952	1.027	0.996	1.123
75	1.287	1.347	1.252	1.367
100	1.360	1.405	1.293	1.411
125	1.337	1.369	1.272	1.274
150	1.276	1.302	1.223	1.310
200	1.134	1.149	1.091	1.152

TABLE 2. Electron-impact ionization cross sections (in 10^{-16} cm^2) of oxygen atoms to form O^+ ions in the $(2p^3)^4S$, ^2D, and ^2P states calculated by the method of exchange distorted waves with Ochkur's approximation (EDWO) and by the Born-Ochkur approximation (BO) in this work at different electron energies E (in eV). Included for comparison are the cross secstions from the earlier works by Burnett and Rountree (BAR) [16], by Peach (PEA) [11,12], by McGuire (MCG), [13] by Omidvar, Kyle, and Sullivan (OKS) [14], and by Kazaks, Ganas, and Green (KGG) [15] as explained in the text. The last five sets of cross sections except PEA were calculated by means of the Born approximation (B) rather than the Born-Ochkur approximation (BO).

	This work						
E(eV)	EDWO	BO	BAR(B)	PEA(BO)	MCG(B)	OKS(B)	KGG(B)
25	0.171	0.326	0.38	0.192	0.55	0.55	
50	0.952	0.996	1.12	0.625	1.15	1.42	2.2
75	1.287	1.367	1.36	0.867	1.35	1.77	2.2
100	1.360	1.293	1.38	0.949	1.48	1.85	2.1
125	1.337	1.272	1.30	0.989	1.48	1.76	1.9
150	1.276	1.223	1.26	0.991	1.44	1.65	1.8
200	1.134	1.091	1.14	0.927	1.26	1.51	1.5
300		0.860		0.790	0.97	1.20	1.2

are more refined than ours. For the initial target state, they used a six-term CI wave function as opposed to our one-configuration Hartree-Fock work. To find the continuum functions for the ejected electron, Burnett and Rountree solved the close-coupling equations icluding the ^4S, ^2D, ^2P term manifold of the $O^+(2p^3)$ configuration whereas in our case the O^+ ion is taken to be in the $(2p^3)^4S$ state. Comparing the cross sections of Burnett and Rountree (BAR), which were calculated by means of the Born approximation, listed in Table 2 with our cross sections calculated by the same method given in the last column of Table 1, we see an agreement within 4%. This supports the accuracy of our wave functions. The cross sections listed under PEA (BO) in Table 2, which were determined by Peach using the BO method, are substantially smaller than our BO results (about 30%). We believe that this is largely due to the different continuum wave functions (for the final target states) used to obtain the two sets of cross sections since the initial target state wave functions are very similar in Peach's and our calculations. In the cases of the MCG, OKS, and KGG calculations (Table 2), the wave functions for both the initial and final target states are different from the ones used in the present work and their cross sections differ from our Born cross sections to varying extents.

Measurements of the ionization cross sections of O atom were reported by Fite and Brackmann (FB) [4]. In a cross-beam experiment, they determined the ratio of the cross sections for ionizing atomic oxygen and molecular oxygen, $\sigma(O^+)/\sigma(O_2{}^+)$. Then utilizing the molecular ionization data of Tate and Smith [8], they obtained $\sigma(O^+)$. In a similar experiment Rothe **et al.**[5] measured ionization cross sections, and their results are in good agreement with those of FB [4]. In the experiment of Brook, Harrison, and Smith (BHS) [6], the charge-exchange process was used as the source of atomic beam so that the absolute cross sections were determined directly. Zipf [7], using the new data of $O_2{}^+$ ionization of Mark [9], revised the cross sections of FB. The "revised" cross sections are smaller than the uncorrected ones by a substantial margin below 100 eV, but above 100 eV the difference is only about 10%. Zipf [7] also determined the cross sections $\sigma(O^+)$ by normalizing his

measurements to the data of BHS and the revised data of FB in the 100-300 eV range. The shape of the ionization function (a plot of cross sections vs incident energy) of Zipf [7] agrees quite well BHS and also with FB above 100 eV.

In Figure 1 we compare the BO and EDWO cross sections of this work with the experimental data of BHS and of FB as revised by Zipf. [7]. The data of Zipf are not included because they are quite close to BHS. The agreement between the present calculation and experiments is seen to be quite good, especially at energies above 70 eV. In the 70-150 eV range the difference is only about 3%, and at 200 eV the present calculation is about 10% smaller than the experimental value. A greater difference is found at lower energies; for example, at 50 eV our value is about 20% smaller than the experimental value. Below 70 eV there exists a substantial difference between the two sets of experimental data shown in Figure 1. Since the BHS data came from a more recent experiment, we use them as the primary source of experimental data for comparison with our calculations. In comparing our calculation with experiments, one must remember that the experimental cross sections include the effects of autoionization as well as the direct ionization, whereas only the latter is considered in the theory. While Brook et al. [6] indicated that their experimental data show no discernible evidence of autoionization, detailed examinations of the ionization yield and optical emission of the autoionizing states [32-34] show that the influence of autoionization on the measured cross sections must be taken into consideration. In particular autoionization via the O [$2s^2 2p^3 (^2P) 3s\,'' \, ^3P^o$] and O [$2s2p^5 \, ^3P^o$] states are found to contribute significantly to the observed ionization cross sections. Since the $^3P^o$ symmetry cannot be realized from the O^+ [$2p^3 \, ^4S$] ion plus an additional (unbound) electron, the autoionization rates of the above-mentioned $^3P^o$ states are much reduced and become comparable to the radiative emission rates. Dehmer et al. [32] experimentally determined the ratio of the autoionization rate to the emission rate to be nearly equal to unity for both the $3s''\, ^3P^o$ and $2s2p^5 \, ^3P^o$ states, i.e., half of the population in these states decay by autoionization and the other half by emission. Zipf and Kao [33], from their experimental emission cross

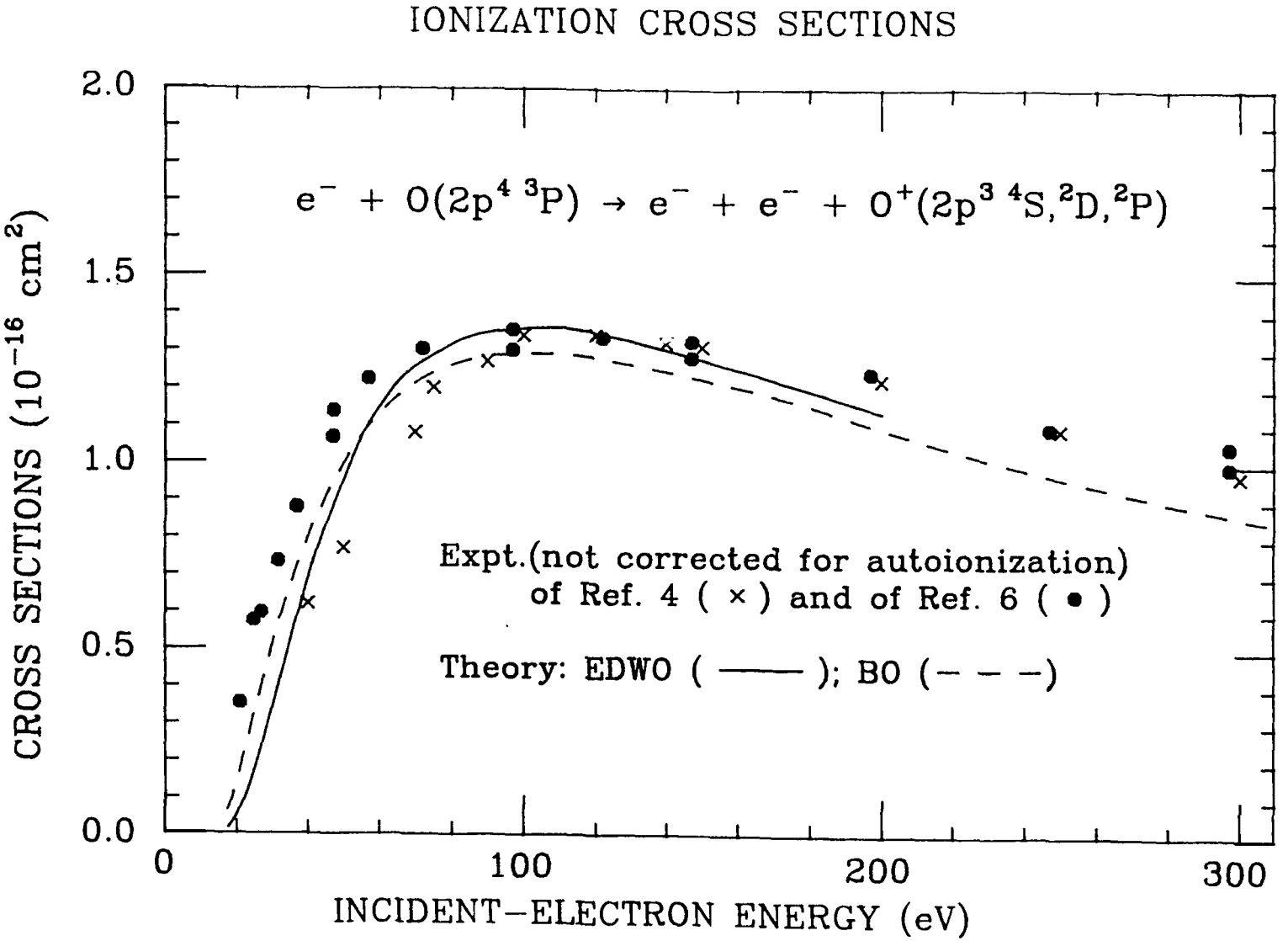

Figure 1. Comparison of the cross sections for electron-impact ionization of the ground-state oxygen atoms calculated by using the EDWO and BO methods with the experimental values that were not corrected for autoionization.

sections and the branching ratios of Dehmer **et al.** [32], conclude that autoionization contributes substantially to the production of $O^+(^4S)$ ions by electron impact. In a more recent electron-impact energy loss experiment, Vaughan and Doering [34] determined the excitation cross sections for several states of atomic oxygen including the two autoionizing $^3P^o$ states mentioned earlier and the $2p^3(^2D)4d'\ ^3P^o$ state at incident-electron energies between 30 and 200 eV. The excitation functions for these states are seen to peak at 50 eV [34]. Applying the branching ratios of Dehmer **et al.** referred to earlier to the excitation cross sections of Vaughan and Doering for the $3s''\ ^3P^o$ and $2s2p^5\ ^3P^o$ states, we can determine the contribution to the ionization cross sections due to autoionization through the $3s''\ ^3P^o$ and $2s2p^5\ ^3P^o$ states. The excitation cross section for the $2p^3(^2D)4d'\ ^3P^o$ state is much smaller than those of the other two $^3P^o$ states mentioned above; thus even if we assume that the $2p^3(^2D)4d'\ ^3P^o$ state decays by autoionization entirely, this autoionization channel makes a much smaller contribution to the measured ionization cross section compared to the $3s''\ ^3P^o$ and $2s2p^5\ ^3P^o$ channels. Indeed Dehmer **et al.** [32] indicated that the $2s^22p^3(^2D)3d'\ ^3P^o$ state decays primarily by autoionization. Thus, we assume a 100% autoionization decay for the $2s^22p^3(^2D)4d'\ ^3P^o$ state in order to determine the contribution from this channel to the ionization cross section. From this analysis we obtain the autoionization contributions to the observed ionization cross sections as 0.068, 0.151, 0.090, 0.071, and 0.048 x 10^{-16} cm^2 at 30, 50, 100, 150, and 200 eV respectively. When this "correction" is made to the measured ionization cross sections of BHS, the agreement between the present theory and experiment is much improved at lower energies as shown in Figure 2. For instance at 50 eV our theoretical value is only 5% smaller than the experimental data, whereas at 100 eV our value is now 8% smaller and at 200 eV 6% larger than the experimental counterparts. At 32 eV, the lowest energy for which we can make the autoionization correction, our theoretical value is 36% lower than the experimental cross section.

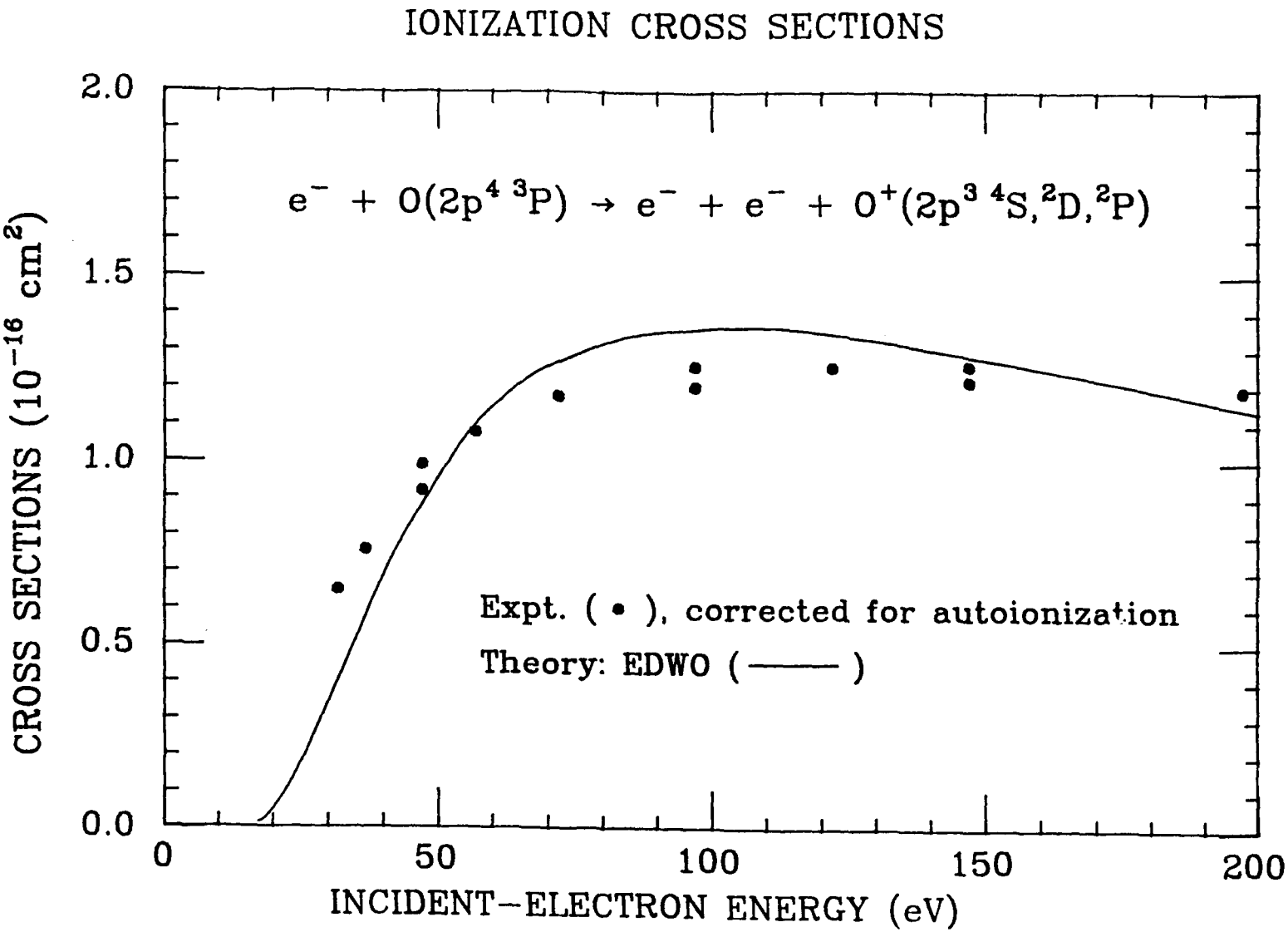

Figure 2. Comparison of the cross sections for electron-impact ionization of the ground-state oxygen atoms calculated by the EDWO method with the experimental data that are corrected for autoionization.

B. Ionization of $O[2p^3(^4S)n_o\ell_o\ ^3L_o]$ to Form $O^+(^4S)$

We have calculated the cross sections for ionizing the excited oxygen atoms $O[2p^3(^4S)n_o\ell_o\ ^3L_o]$ by electron impact. In Figures 3 and 4, we show the BO and EDWO cross sections for $n_o\ell_o$ = 3s, 3p, and 3d. In each case the peak of the ionization function occurs immediately above the threshold (8.0 eV for 3s, 6.0 eV for 3p, and 4.0 eV for 3d), in marked contrast to ionization of the ground state where the peak cross section occurs at about 100 eV. Such a characteristic distinction between ionization from the ground state and from excited states is also seen for the H and He atoms. The ionization functions for H(2s) and H(2p) peak around 8-13 eV [30], whereas the maximum of the H(1s) ionization function occurs within 80-100 eV. Similarly the ionization functions for $He(2^1S)$ and $He(2^3S)$ peak around 10 eV [35], as opposed to the peak position in the 80-100 eV range for He(1s) [36]. As in the case of ionization from the ground state, the EDWO cross sections are substantially smaller than the BO cross sections at low energies. However, the two sets of cross sections become much closer to each other with increasing energy as can be seen in Table 3.

We have extended the BO calculation to $n_o\ell_o$ up to (6,5). The general shape of the ionization function remains the same except for a small inward shift in the peak. We have fitted the ionization function for each $n_o\ell_o$ from 7.5 eV to 500 eV to the relation

$$\sigma = c_1 E^{-1} lnE + c_2 E^{-1} + c_3 E^{-2}, \tag{45}$$

where the incident-electron energy E is in eV and the cross section in cm^2. The numerical values of c_1, c_2, and c_3 are given in Table 4.

Finally it should be recalled that in the present calculation the initial states are triplet states. Although we did not make a separate set of calculations for the case of quintet initial states, we expect the latter cross sections to be rather close to the former set. In the radiative-recombination calculation [28] involving the above two sets of triplet and quintet states, the difference in cross sections were found to be about 15% for n_o = 3, 10% for n_o = 4, and less still for higher n_o.

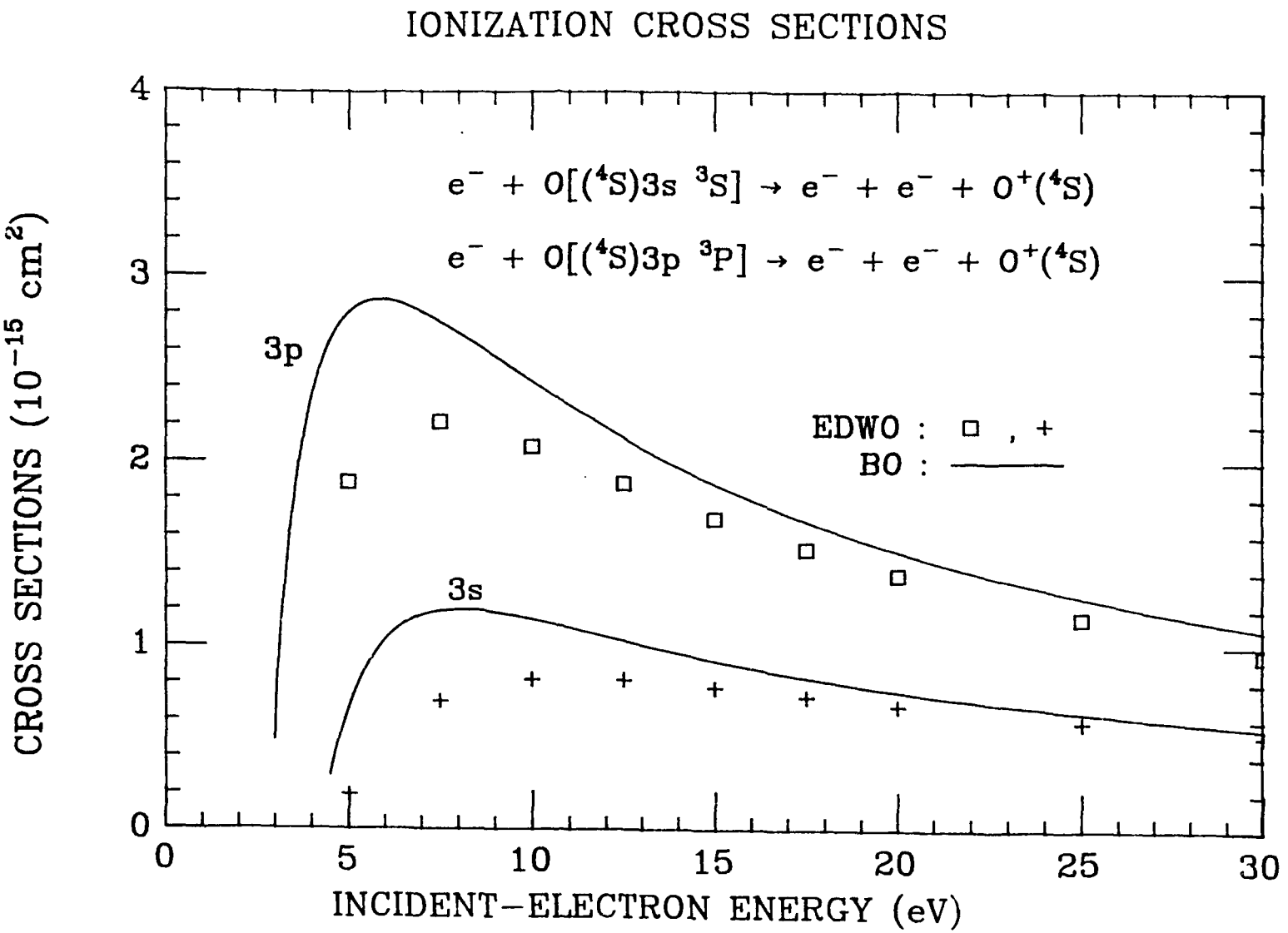

Figure 3. Cross sections for electron-impact ionization of oxygen atom in the $[2p^3(^4S)3s]^3S$ and $[2p^3(^4S)3p]^3P$ states calculated by the BO method (solid curves) and by the EDWO method (□ and +).

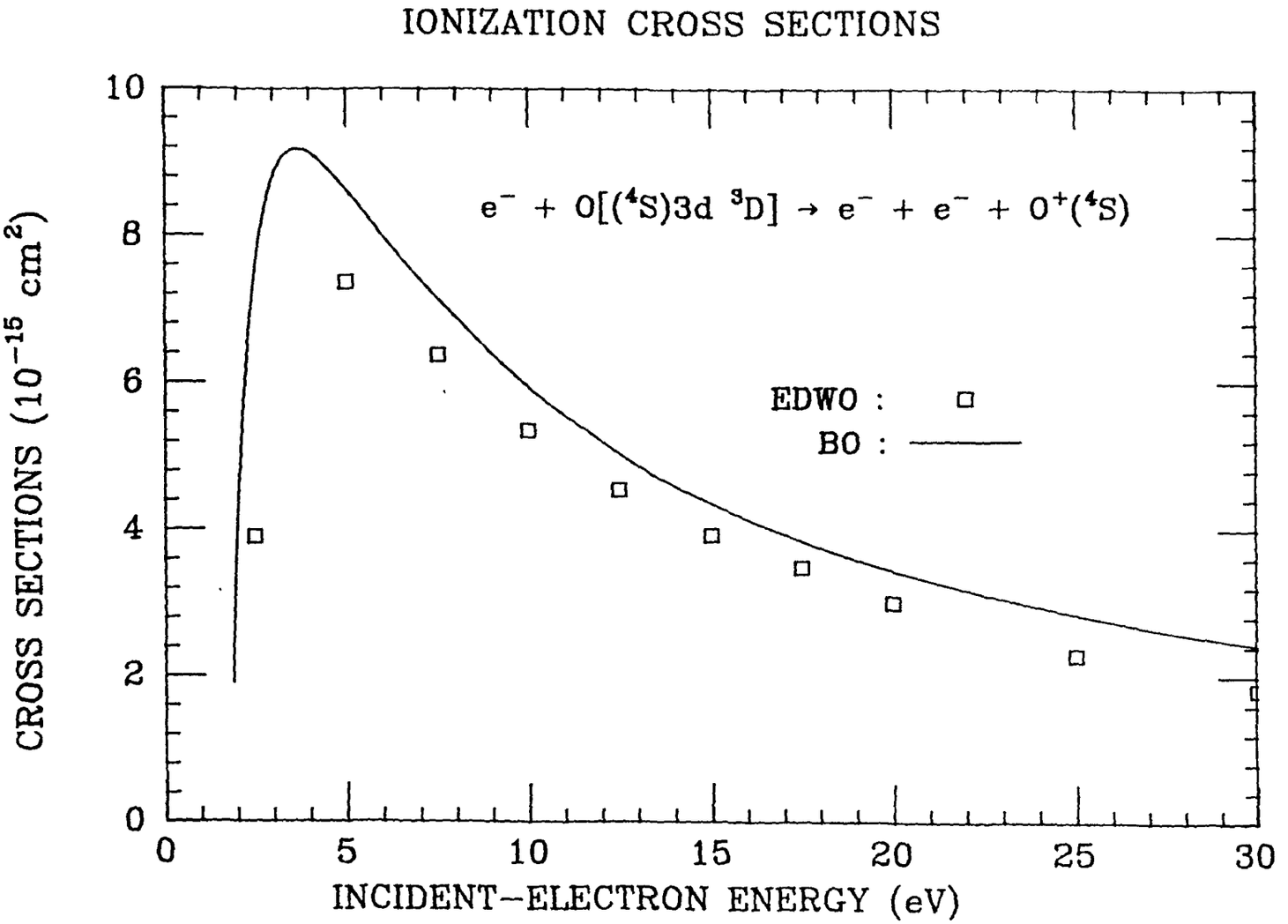

Figure 4. Cross sections for electron-impact ionization of oxygen atoms in the $[2p^3(^4S)3d]^3D$ state calculated by the BO method (solid curve) and by the EDWO method (□).

TABLE 3. Comparison of the BO and EDWO cross sections for ionization of oxygen atoms in the $[2p^3(^4S)n_o\ell_o]^3L_o$ states. For each incident-electron energy E, there are two entries: the first is the BO and the second the EDWO cross sections (in 10^{-15} cm^2).

E(eV)	3s	3p	3d
2.5			7.49
			3.90
5.0	0.659	2.80	8.62
	0.189	1.88	7.36
7.5	1.19	2.75	7.14
	0.700	2.21	6.37
10.0	1.14	2.43	5.93
	0.818	2.08	5.34
12.5	1.02	2.12	5.03
	0.815	1.88	4.54
15.0	0.917	1.88	4.36
	0.774	1.69	3.93
17.5	0.827	1.68	3.85
	0.724	1.53	3.49
20.0	0.752	1.51	3.44
	0.674	1.39	3.00

TABLE 4. Values of the coefficients in the Bethe-type expansion [Eq. (45)] of the ionization cross sections (in cm^2) for the oxygen atoms in the $[2p^3(^4S)n_o\ell_o]^3L_o$ states as a function of the incident-electron energies (in eV).

n_o,ℓ_o	c_1	c_2	c_3
3,0	1.135[-15][a]	1.458[-14]	-5.797[-14]
4,0	2.682[-15]	4.172[-14]	-7.230[-14]
5,0	3.760[-15]	8.517[-14]	-8.563[-14]
6,0	1.473[-15]	1.480[-13]	-1.096[-13]
3,1	1.541[-15]	3.044[-14]	-9.684[-14]
4,1	7.842[-15]	5.170[-14]	-5.615[-14]
5,1	1.522[-14]	9.016[-14]	-5.832[-14]
6,1	1.709[-14]	1.458[-13]	-5.230[-14]
3,2	4.265[-15]	6.280[-14]	-13.380[-14]
4,2	1.354[-14]	8.649[-14]	-6.529[-14]
5,2	2.437[-14]	1.202[-13]	-3.767[-14]
6,2	1.627[-14]	2.028[-13]	-6.385[-14]
4,3	7.231[-15]	1.084[-13]	-9.185[-14]
5,3	1.688[-14]	1.444[-13]	-6.222[-14]
6,3	1.791[-14]	2.013[-13]	-5.938[-14]
5,4	7.499[-15]	1.696[-13]	-8.738[-14]
6,4	1.088[-14]	2.239[-13]	-7.515[-14]
6,5	7.535[-15]	2.309[-13]	-7.217[-14]

[a]Number inside the brackets indicates the power of 10.

4. SUMMARY AND CONCLUSIONS

We have calculated the electron-impact ionization cross sections of producing the O^+ ions (in the $2p^3$ configuration) from the ground state $O(^3P)$ atom by the BO and by EDWO approximations. For comparison similar calculations neglecting electron exchange have been performed (the B and DW approximations). The continuum wave functions of the ionized electron were computed by the HF method with full allowance for the Coulomb and exchange interactions with the remaining electrons and the nucleus of O^+.

The EDWO gives significantly smaller cross sections than does BO at low electron energies. For example, at 30 eV the EWDO cross section is smaller by 15%, and at lower energy smaller still by a greater percentage. However, between 70-200 eV, the difference is about 10% or less, and the two sets of cross sections tend to merge at high incident energy.

By accounting for the distortion of the projectile electron by the target and using the proper continuum functions, we made a significant improvement over the previous calculations, which are within the stage of the B or BO approximation and, in most cases, with the hydrogenic Coulomb functions, so that we can make a quantitative comparison with the experimental measurements [4-7]. In the energy range of 50-200 eV the present EDWO cross sections agree with the experimental measurements (with correction for autoionization contributions) within about 10% or less. Below 50 eV the discrepancy becomes larger. For instance at 32 eV our EDWO cross section is 36% below the experimental value. One may speculate that the larger discrepancy at low energies may be partly due to a possible increase in the percentage uncertainty of the experimental measurements on account of the cross sections being much smaller and varying steeply with energy. It should also be pointed out that in our BO and EDWO calculations, the polarization of the target-state wave functions by the incident electron is neglected. This target polarization effect is more important at very low incident-electron energies, and may be partly responsible for the discrepancy between theory and experiment at very low energies. We may also add that at energies above 37 eV, ionization may take place through channels in which the O^+ ion is initially formed in

an excited configuration such as $2p^23s$. However, contributions from these channels, which involve two active electrons and are not included in our calculations, to the ionization cross sections are unimportant when we are discussing accuracy on the level of 10%.

We have computed BO cross sections of ionizing Rydberg oxygen atoms in the $[2p^3(^4S)n_o\ell_o]^3L_o$ for $(n_o\ell_o) = (3,0)$ through $(n_o\ell_o) = (6,5)$. These cross sections are sharply peaked within a few eV above the threshold in contrast to the ionization function of the ground state, which shows a broad peak around 100 eV. Similar characteristic distinction between ionization of the ground state and excited states has also been reported for the H and He atoms. For comparison we have used the EDWO approximation to calculate the ionization cross sections for the Rydberg oxygen atoms with $n_o = 3$. The EDWO cross sections are significantly smaller than their BO counterparts at low incident energies but above 15 eV or so the two sets become quite close to each other.

To summarize the large amount of the BO ionization cross section data for the Rydberg oxygen atoms, we present the cross sections in the form of a Bethe-type expansion. Detailed information about ionization processes involving excited oxygen atoms is important in studies of radiation in the upper atmosphere and in modeling and diagnostics of plasmas.

REFERENCES

1. "Electron impact ionization cross-section data for atoms, atomic ions, and diatomic molecules: I. experimental data," L.J. Kieffer and G. H. Dunn, Rev. Mod. Phys. **38**, 1 (1966).

2. "Updated excitation and ionization cross sections for electron impact on atomic oxygen," R. R. Laher and F. R. Gilmore, J. Phys. Chem. Ref. Data **19**, 277 (1990).

3. "Recommended data on the electron impact ionization of atoms and ions," K. L. Bell, H. B. Gilbody, J. G. Hughes, A. E. Kingston, and F. J. Smith, J. Phys. Chem. Ref. Data, **12**, 891 (1983).

4. "Ionization of atomic oxygen on electron impact," W. L. Fite and R. T. Brackmann, Phys. Rev. **113**, 815 (1959).

5. "Electron impact ionization of atomic hydrogen and atomic oxygen," E. W. Rothe, L. L. Marino, R. H. Neynaber, and S. M. Trujillo, Phys. Rev. **125**, 582 (1962).

6. "Measurements of the electron impact ionization cross sections of He, C, O and N Atoms," E. Brook, M. F. A. Harrison, and A. C. H. Smith, J. Phys. B **11**, 3115 (1978).

7. "The ionization of atomic oxygen by electron impact," E. C. Zipf, Planet. Space Sci., **33**, 1303 (1985).

8. "The efficiencies of ionization and ionization potentials of various gases under electron impact," J. T. Tate and P. T. Smith, Phys. Rev. **39**, 270 (1932).

9. "Cross section for single and double ionization of N_2 and O_2 molecules by electron impact from threshold up to 170 eV," T. D. Mark, J. Chem. Phys. **63**, 3731 (1975).

10. "Electron impact ionization of Ne, O, and N," M. J. Seaton, Phys. Rev. **113**, 814 (1959).

11. "Ionization of neutral atoms with outer 2p and 3p electrons by electron and proton impact," G. Peach, J. Phys. B **1**, 1088 (1968).

12. "Ionization of atoms and positive ions by electron and proton impact," G. Peach, J. Phys. B **4**, 1670 (1971).

13. "Inelastic scattering of electrons and protons by elements He to Na," E. J. McGuire, Phys. Rev. A **3**, 267 (1971).

14. "Ionization of multielectron atoms by fast charged particles," K. Omidvar, H. L. Kyle, and E. C. Sullivan, Phys. Rev. A **5**, 1174 (1972).

15. "Electron-impact excitation and ionization of atomic oxygen," P. A. Kazaks, P. S. Ganas, and A. E. S. Green, Phys. Rev. **A6**, 2169 (1972).

16. "Differential and total cross sections for electron-impact ionization of atomic oxygen," T. Burnett and S. P. Rountree, Phys. Rev. **A20**, 1468 (1979).

17. E. Clementi, **Tables of Atomic Wave Functions** (San Jose, California: IBM, 1965).

18. "Ionization of the hydrogen atom by electron impact with allowance for the exchange," V. I. Ochkur, Sov. Phys. JETP **20**, 1175 (1965).

19. "Roothaan-Hartree-Fock atomic wavefunctions basis functions and their coefficients for ground and certain excited states of neutral and ionzied atoms, $Z \leq 54$," E. Clementi and C. Roetti, At. Data Nucl. Data Tables **14**, 177 (1974).

20. R. K. Peterkop, **Theory of Ionization of Atoms by Electron Impact,** (Colorado Associated University Press, 1977).

21. "The threshold low for ionizing collisions," M. R. H. Rudge and M. J. Seaton, Proc. Phys. Soc. Lond. **83**, 680 (1964); "Ionization of atomic hydrogen by electron impact," M. R. H. Rudge and M. J. Seaton, Proc. Roy. Soc. **A283**, 262 (1965).

22. "Theory of the ionization of atoms by electron impact," M. R. H. Rudge, Rev. Mod. Phys. **40**, 564 (1968).

23. "Theory of (e,2e) reactions," F. W. Byron Jr. and C. J. Joachain, Phys. Rep. **179**, 211 (1989); "Excitation of atomic positive ions by electron impact,"R. J. W. Henry, Phys. Rep. **68**, 1 (1980).

24. Electron-impact ionization cross sections for highly ionized hydrogen- and lithium-like atoms," S. M. Younger, Phys. Rev. A **22**, 111 (1980).

25. "Triple-differential cross sections for electron-impact ionization of helium," D. H. Madison, R. V. Calhoun, and W. N. Shelton, Phys. Rev. A**16**, 552 (1977); "Distorted-wave-method calculation of electron-impact excitation of atomic ions: He- and Be-like ions," Y. Itikawa and K. Sakimoto, Phys. Rev. A**31**, 1319 (1985).

26. E. U. Condon and G. H. Shortley, **The Theory of Atomic Spectra** (Cambridge Press; 1963), p. 175.

27. "Transition probabilities of OI spectral lines," S. Chung, C. C. Lin, and E. T. P. Lee, J. Quant. Spectrosc. Radiat. Transfer **36**, 19 (1986).

28. "Radiative-recombination cross sections and rate coefficients of atomic oxygen," S. Chung, C. C. Lin, and E. T. P. Lee, Phys. Rev. A **43**, 3433 (1991).

29. B. W. Shore and D. H. Menzel, **Principles of Atomic Spectra** (John Wiley and Sons, NY 1968), pp. 378-91.

30. "Ionization of H(2s) and H(2p) by electron impact," S. S. Prasad, Proc. Phys. Soc. **87**, 393 (1966).

31. "Analytic independent-particle model for atoms," A. E. S. Green, D. L. Sellin, and A. S. Zachor, Phys. Rev. **184**, 1 (1969).

32. "Competion between autoionization and radiative emission in the decay of excited states of the oxygen atom," P. M. Dehmer, W. L. Luken, and W. A. Chupka, J. Chem. Phys. **67**, 195 (1977).

33. "Electron-impact excitation of the 3s"$^3P^o$ and $2s2p^5$ $^3P^o$ autoionizing states of atomic oxygen," E. C. Zipf and W. W. Kao, Chem. Phys. Lett. **125**, 394 (1986).

34. "Absolute experimental differential and integral electron excitation cross sections for atomic oxygen 4. The ($^3P \rightarrow 3s"$ $^3P^o$), ($^3P \rightarrow 2s2p^5$ $^3P^o$), ($^3P \rightarrow 4d'^3P^o$) autoionizing transitions (878, 792, and 770 $\AA$) and five members of the ($^3P \rightarrow$ nd $^3D^o$), Rydberg series (1027$\AA$)," S. D. Vaughan and J. P. Doering, J. Geophys. Res. **93**, 289 (1988).

35. "Cross sections for excitation and ionization in e-He($2^{1,3}S$) collisions," D. Ton-That, S. T. Manson, and M. R. Flannery, J. Phys. B **10**, 621 (1977).

36. "The ionization of helium by high energy electrons," K. L. Bell and A. E. Kingston, J. Phys. B **2**, 1125 (1969).

PART 2

THREE-BODY RECOMBINATION OF ELECTRONS WITH ATOMIC OXYGEN IONS

The three-body recombination of electrons with atomic oxygen ion to form an excited oxygen atom in the $2p^3(^4S)n\ell\ ^3L$ state,

$$e^- + e^- + 0^+ \left[2p^3(^4S)\right] \rightarrow e^- + 0\left[2p^3(^4S)nl\,^3L\right], \tag{46}$$

is the inverse process of electron-impact ionization,

$$e^- + 0\left[2p^3(^4S)nl\,^3L\right] \rightarrow e^- + e^- + 0^+ \left[2p^3(^4S)\right] \tag{47}$$

discussed in Part 1. With the electron-impact ionization cross sections at various incident energies obtained in Part 1, we can calculate the ionization rate coefficients and the three-body recombination constants.

Consider an oxygen atom initially in the $2p^3(^4S)n\ell\ ^3L$ state, which we designate as state "p", colliding with an electron of velocity v and resulting in ionization with the ejected electron in a continuum state "c". If we denote the cross section for this process as $\sigma_p(v)$, the ionization coefficient at temperature T corresponding to the p→c ionization process is

$$K(p \rightarrow c; T) = \int_{v_o}^{\infty} v\sigma_p(v) f(v,T) dv, \tag{48}$$

where $f(v,T)$ is the Maxwell-Boltzmann distribution function,

$$f(v,T) = 4\pi(m/2\pi kT)^{3/2} exp(-mv^2/2kT), \tag{49}$$

and v_o is the threshold incident velocity for the $p \rightarrow c$ ionization. Since we have already determined the ionization cross section $\sigma_p(v)$ in Part 1, the ionization rate coefficient can be calculated as a function of temperature from Eq. (48).

The three-body recombination constant is denoted by $K(c \rightarrow p; T)$ and is related to the ionization coefficient through the equilibrium constant $K_{eq}(T)$ as

$$K(c \rightarrow p; T) = K(p \rightarrow c; T)/K_{eq}(T), \tag{50}$$

$$K_{eq}(T) = 2(g_+/g_p)(2\pi mkT/h)^{3/2} exp(-I_p/kT), \tag{51}$$

where g_+ and g_p are the degeneracies of the atomic ion and the state "p" of the atom respectively, and I_p is the ionization energy of the state "p". Note that the ionization rate coefficient is customarily expressed in units of cm^3/s. The equilibrium constant K_{eq} is in $(length)^{-3}$, so that the three-body recombination rate constant $K(c \rightarrow p; T)$ is expressible in units cm^6/s.

The ionization rate coefficients of the ground-state oxygen atom are computed with the cross sections obtained by the exchange-distorted-waves method with Ochkur's approximation (EDWO) as described in Part 1. The results are shown in Figure 5. For the oxygen atoms in triplet excited states $2p^3(^4S)n\ell\ ^3L$ (with $n \geq 3$), the ionization rate coefficients are calculated with the Born-Ochkur cross sections and the results are shown in Figures 6-9. Although we have not computed the cross sections for the quintet states, i.e., $2p^3(^4S)n\ell\ ^5L$, then cross sections are expected to be very close to the cross sections for the triplet counterparts. In the radiative combination process, the cross sections of capture into the triplet and quintet states are quite close [1].

The three-body recombination constants have been calculated from Eq. (50) and the results are shown in Figures 10-14. We found that the temperature dependence for the three-body recombination constants for the excited states of oxygen can be fitted to the form

$$K(c \rightarrow p; T) = aT^{-\eta} \tag{52}$$

in two regions of electron temperature T; $5x10^3$ - $2x10^4$ °K and $2x10^4$ - $2x10^5$ °K. The parameters a and η are shown in Table 5. In all cases Eq. (52) reproduces the original values to with 10% and usually much better.

In the past classical formulas have been used to calculate the ionization cross sections from which one can obtain the three-body recombination constants and the ionization rate coefficients [2]. For instance the classical formula of Thomson gives the ionization cross

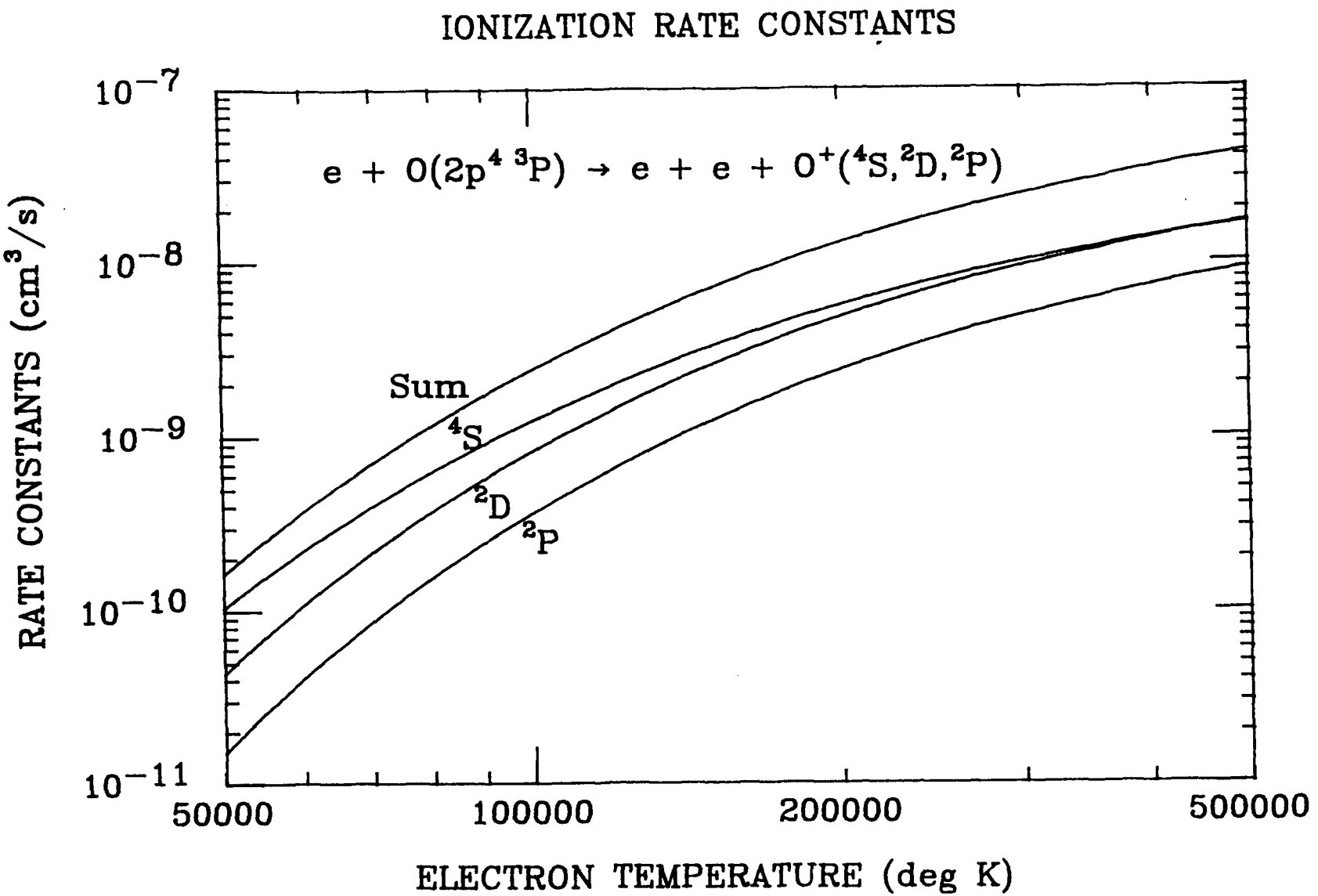

Figure 5. Ionization rate constants at various electron temperatures for ionizing oxygen atoms in the $2p^4(^3P)$ ground state to the $O^+(^4S)$, $O^+(^2D)$, and $O^+(^2P)$ ions.

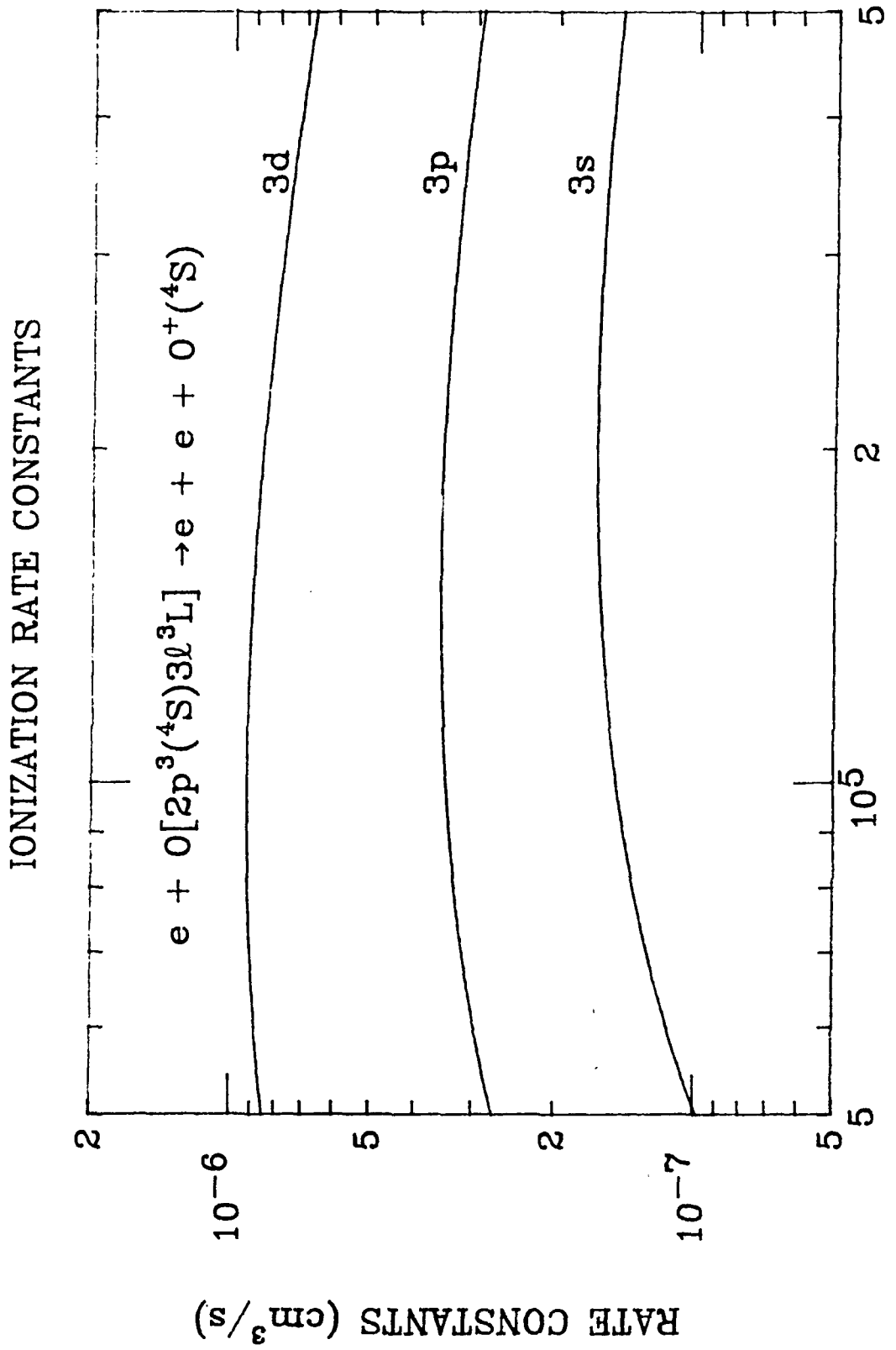

Figure 5. Ionization rate constants at various electron temperatures for ionizing oxygen atoms in the $[2p^3(^4S)3\ell]^3L$ excited states with 3ℓ=3s, 3p, and 3d.

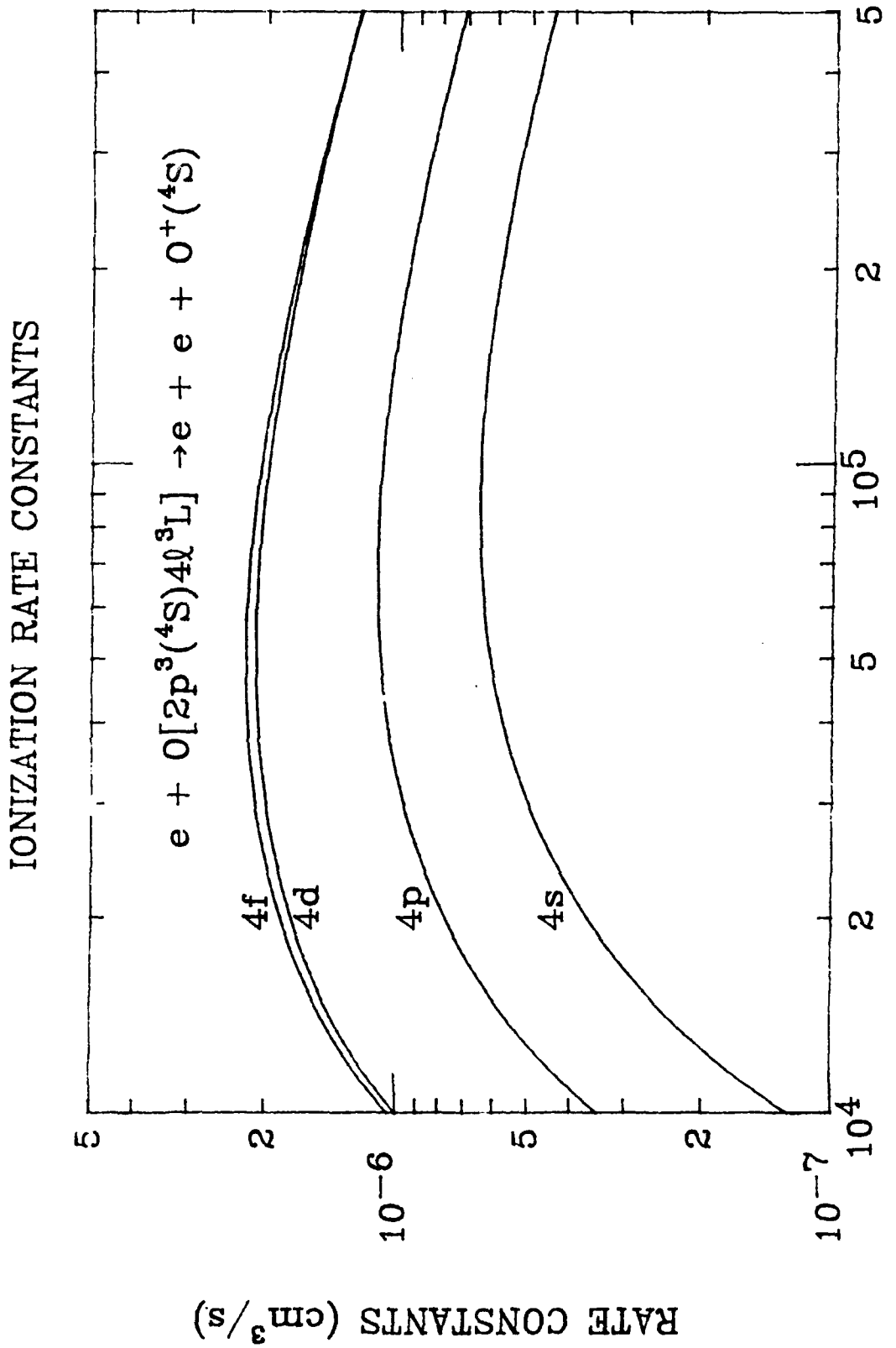

Figure 7. Ionization rate constants at various electron temperatures for ionizing oxygen atoms in the $[2p^3(^4S)4\ell^3]^3L$ excited states with 4ℓ=4s, 4p, 4d, and 4f

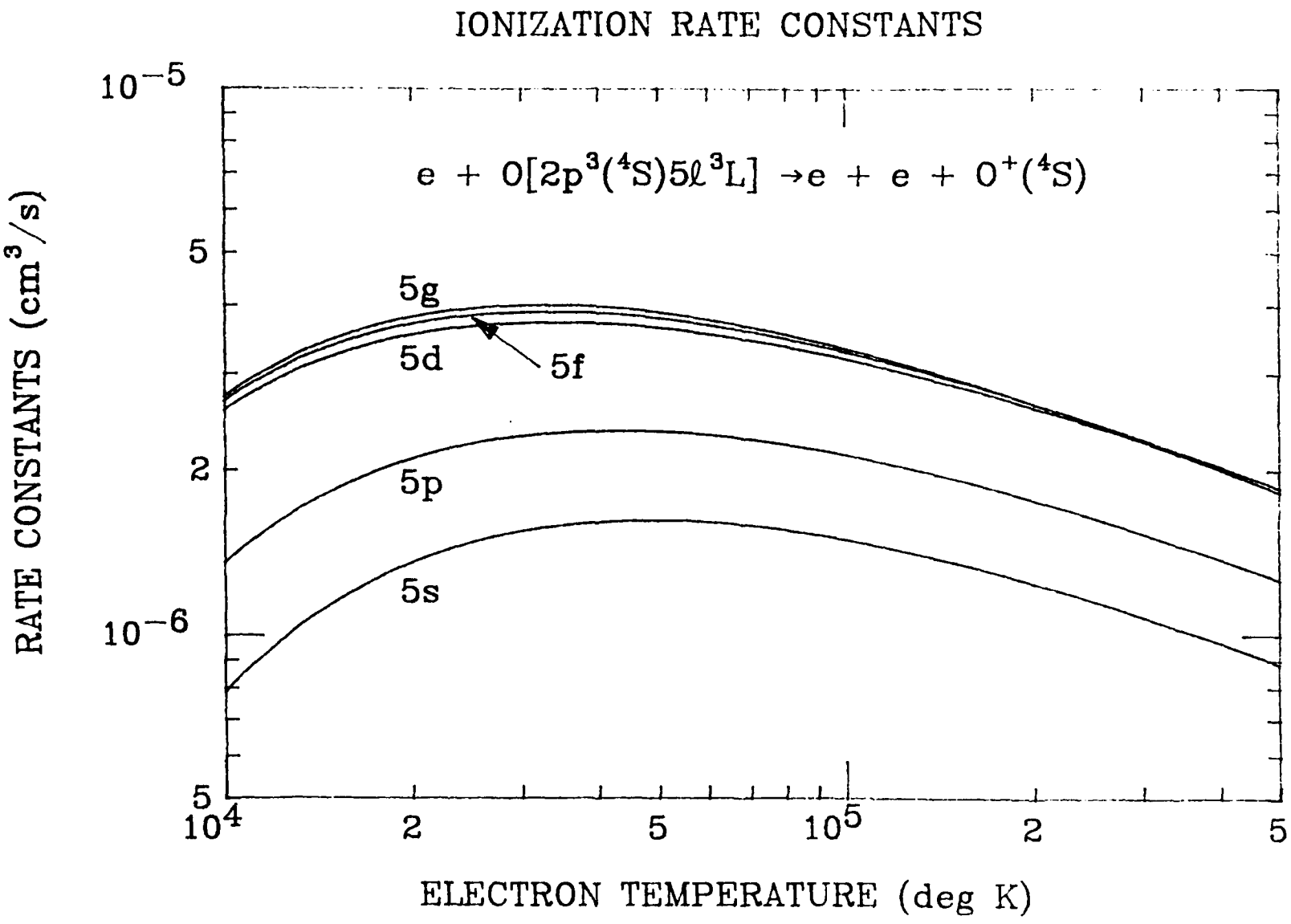

Figure 8. Ionization rate constants at various electron temperatures for ionizing oxygen atoms in the $[2p^3(^4S)5\ell]^3L$ excited states with $n\ell$=5s, 5p, 5d, 5f, and 5g.

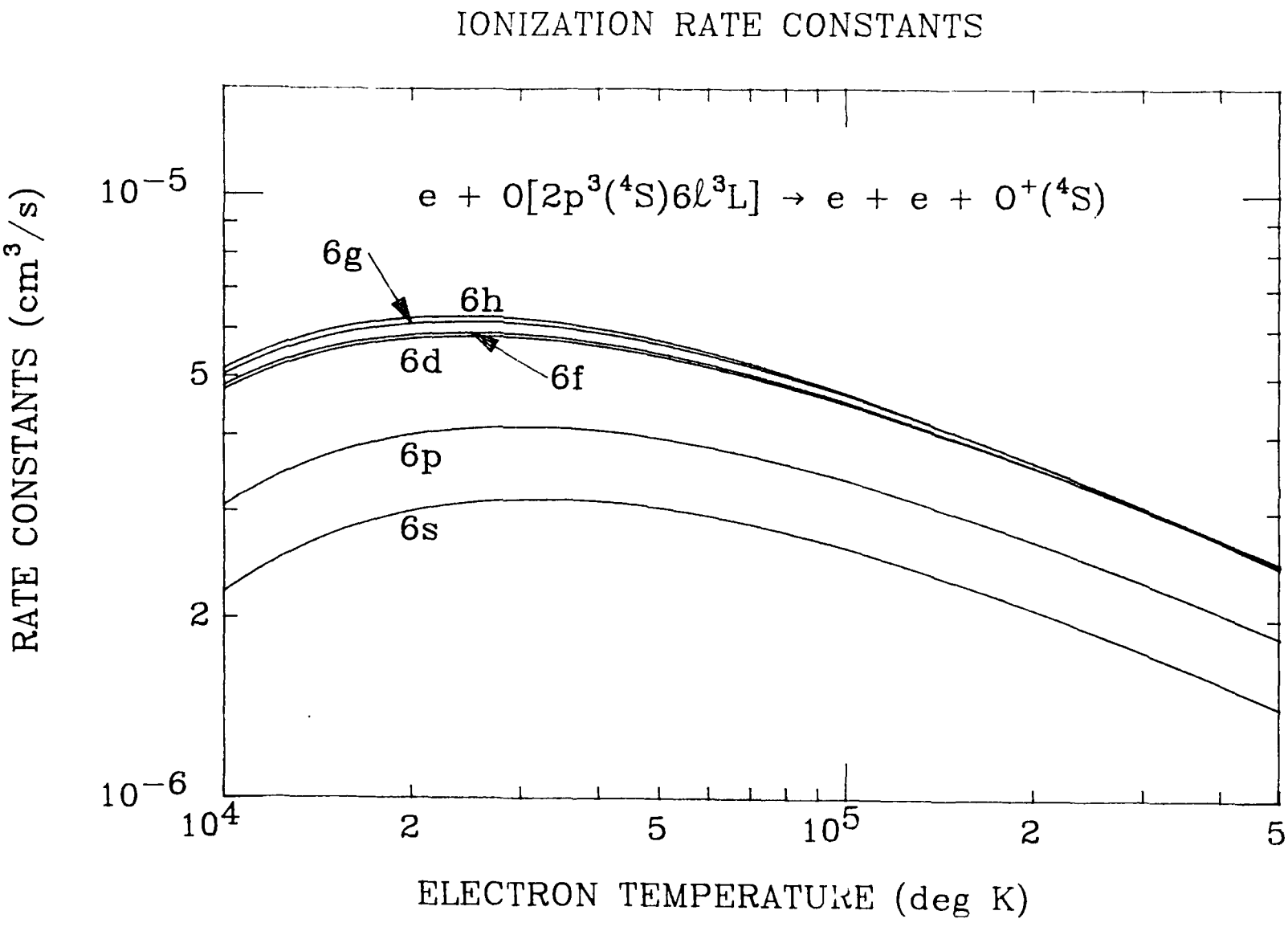

Figure 9. Ionization rate constants at various electron temperatures for ionizing oxygen atoms in the $[2p^3(^4S)6\ell]^3L$ excited states with 6ℓ=6s, 6p, 6d, 6f, 6g, and 6h.

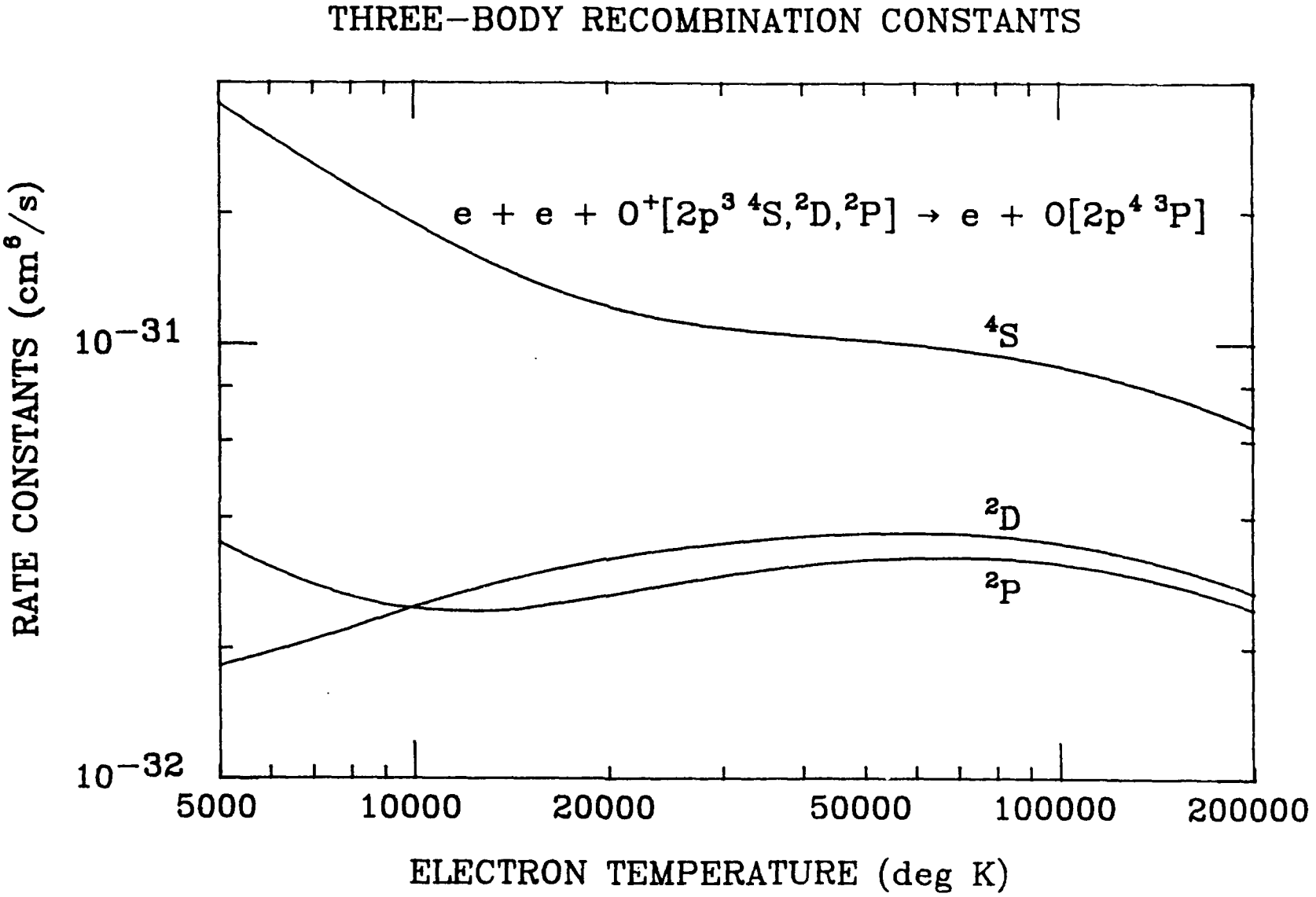

Figure 10. Three-body recombination constants at various temperatures for $O^+(^4S)$, $O^+(^2D)$, and $O^+(^2P)$ recombining with electrons to form $O[2p^4(^3P)]$ atoms.

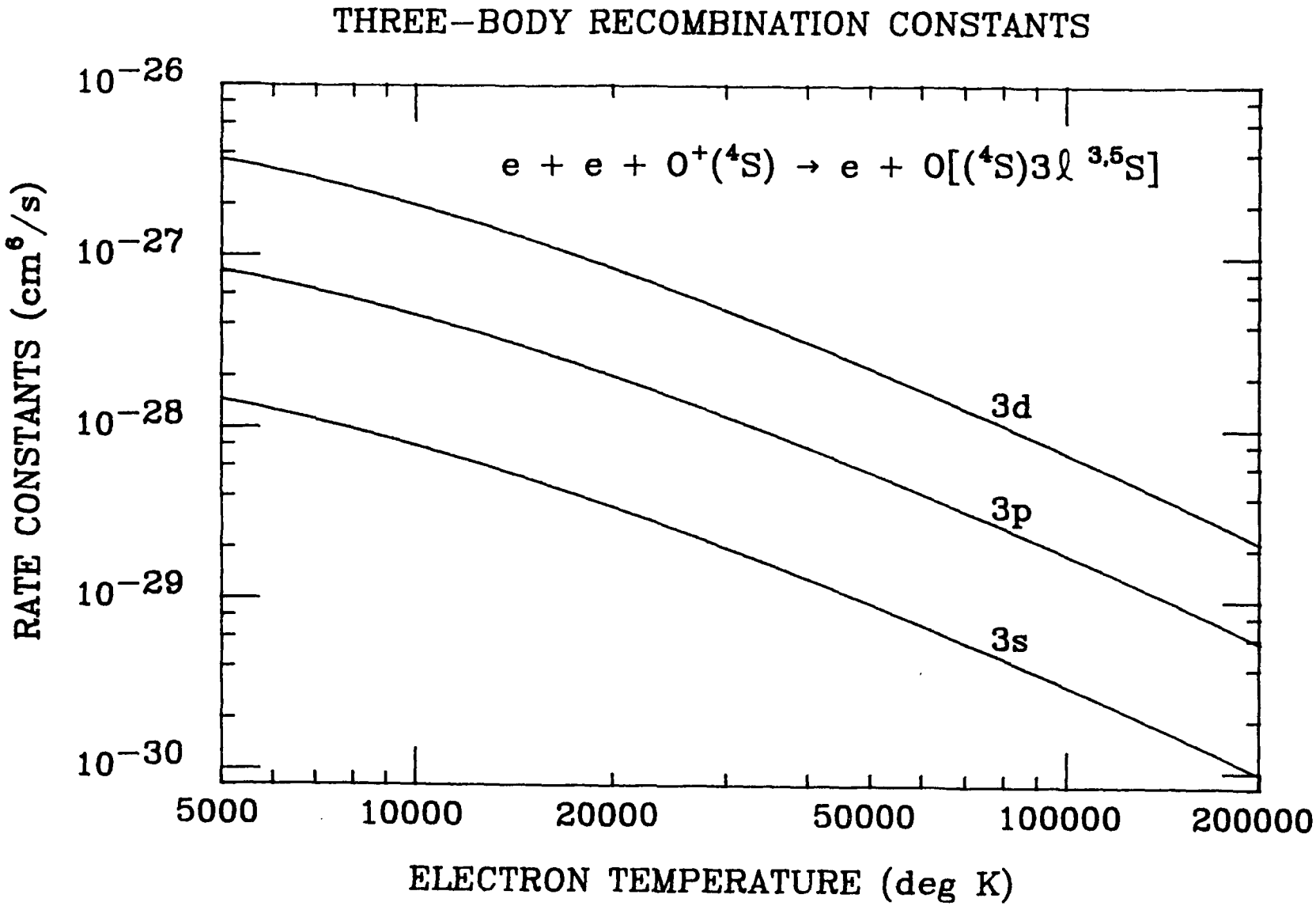

Figure 11. Three-body recombination constants at various temperatures for $O^+(^4S)$ recombining with electrons to form oxygen atoms in the $[(^4S)3\ell]^3L$ excited states with 3ℓ=3s, 3p, and 3d.

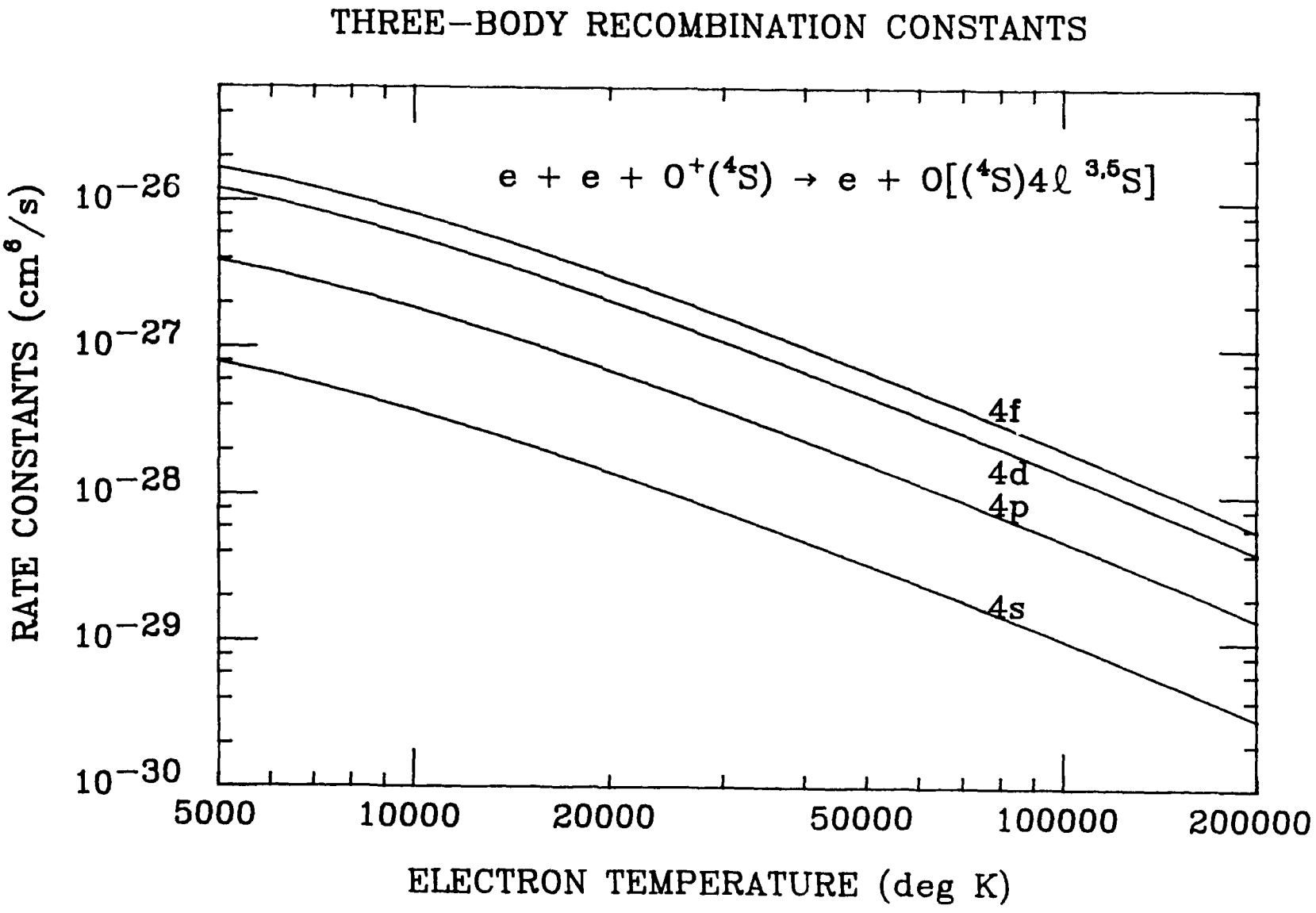

Figure 12. Three-body recombination constants at various temperatures for $O^+(^4S)$ recombining with electrons to form oxygen atoms in the $[(^4S)4\ell]^3L$ excited states with 4ℓ=4s, 4p, 4d, and 4f.

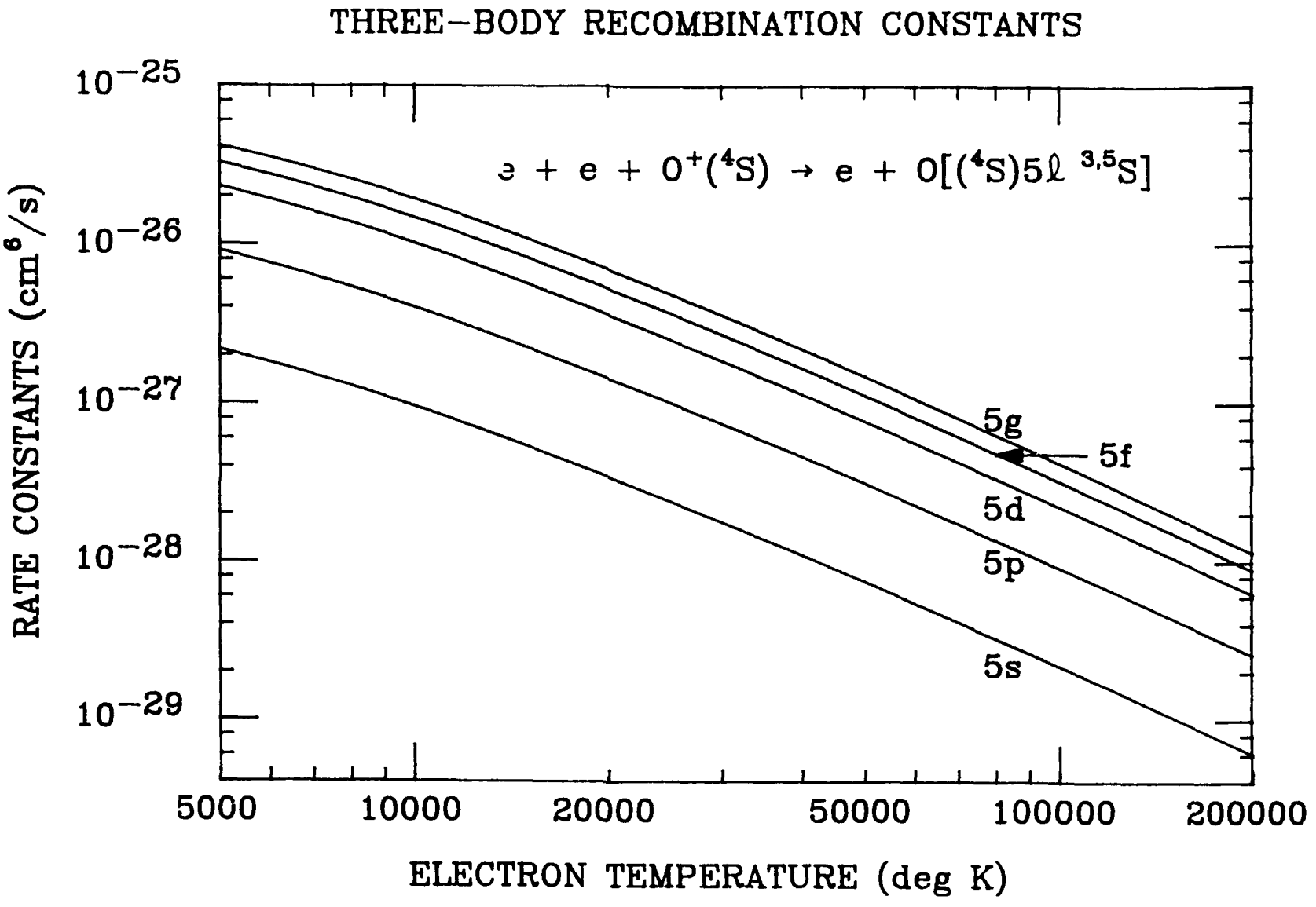

Figure 13. Three-body recombination constants at various temperatures for $O^+(^4S)$ recombining with electrons to form oxygen atoms in the $[(^4S)5\ell]\ ^3L$ excited states with 5ℓ=5s, 5p, 5d, 5f, and 5g.

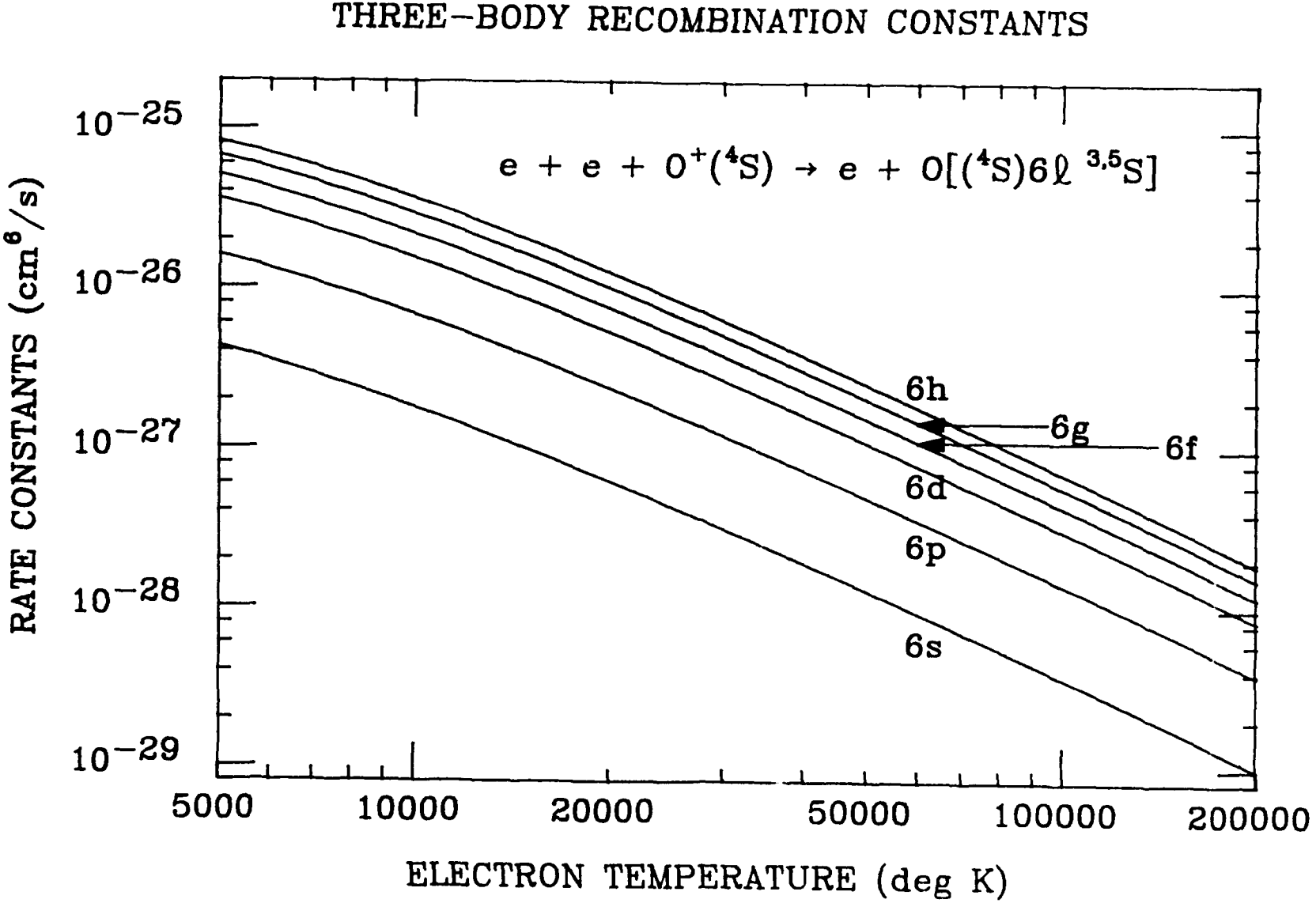

Figure 14. Three-body recombination constants at various temperatures for $O^+(^4S)$ recombining with electrons to form oxygen atoms in the $[(^4S)6\ell]^{3,5}L$ excited states with 6ℓ=6s, 6p, 6d, 6f, 6g, and 6h.

Table 5. Values of a and η in $K(c \rightarrow p; T) = aT^{-\eta}$ for two different temperature regions.

State	T = 5x10^3 - 2x10^4 °K		T = 2x10^4 - 2x10^5 °K	
	a	η	a	η
3s	1.134[-24][a]	1.044 999	1.806[-22][a]	1.553 714
3p	5.446[-24]	1.025 274	1.015[-21]	1.549 876
3d	3.406[-23]	1.064 035	6.800[-20]	1.596 219
4s	3.328[-23]	1.243 110	2.538[-21]	1.679 510
4p	1.642[-22]	1.242 221	1.516[-20]	1.698 688
4d	6.520[-22]	1.271 318	5.305[-20]	1.715 270
4f	6.287[-22]	1.227 865	9.058[-20]	1.729 279
5s	2.250[-22]	1.348 549	1.193[-20]	1.748 639
5p	9.654[-22]	1.351 053	4.800[-20]	1.745 048
5d	2.663[-21]	1.360 183	1.385[-19]	1.759 402
5f	3.134[-21]	1.337 922	2.304[-19]	1.771 964
5g	3.176[-21]	1.310 384	3.499[-19]	1.785 248
6s	7.302[-23]	1.470 302	3.356[-20]	1.793 332
6p	2.315[-21]	1.387 725	1.236[-19]	1.789 453
6d	5.457[-21]	1.392 790	3.057[-19]	1.779 628
6f	7.718[-21]	1.392 499	4.534[-19]	1.804 076
6g	9.429[-21]	1.382 759	6.855[-19]	1.815 851
6h	1.090[-20]	1.374 620	9.474[-19]	1.825 962

[a]The number inside the bracket indicates the power of 10.

section σ(E) at incident electron E as

$$\sigma(E) = \left(\pi e^4\right)\left(E_p^{-1} - E^{-1}\right), \tag{53}$$

where E_p is the ionization energy of state "p". For comparison we have computed the three-body recombination constants by means of this classical empirical procedure. In applying Eq. (53) to calculate the ionization cross sections, we use the experimental value of E_p rather than the hydrogenic value. The resulting classical values for the three-body recombination constants are larger than the quantum-mechanical counterparts at low electron temperature. For example at 5000°K the classical values are larger by as much as 20%. Conversely at 100,000°K, the classical values are smaller than quantum-mechanical ones by as much as 35%.

REFERENCES

1. "Radiative-recombination cross sections and rate coefficients of atomic oxygen," S. Chung, C. C. Lin, and E. T. P. Lee, Phys. Rev. A**43**, 3433 (1991).

2. See, for example, Ya. B. Zel'dovich and Yu. P. Raizer, "Physics of Shock Waves and High-Temperature Hydrodynamic Phenomena" (Academic Press, New York 1966), Vol. I, Chap. 16.

PART 3

ELECTRONIC STRUCTURE OF THE HIGHLY EXCITED STATES OF THE OXYGEN MOLECULE

Rydberg-state wave functions that converge to the O_2^+ ground state have been calculated for five difference values of the internuclear distance R (1.0, 1.117, 1.207, 1.3, and 1.4 $\AA$) for the total molecular symmetry of $O_2^+(X^2\Pi_g)(n\ell)^{1,3}\Pi_{g,u}$ for $(n\ell)$ from (3,0) to (10,9) by a Hartree-Fock scheme in which the Coulomb and exchange interaction of the Rydberg electron with the O_2^+ core is treated rigorously. The wave function of the $O_2^+(X^2\Pi_g)$ ion core is obtained by a multiconfiguration self-consistent field method. Comparison of the vertical excitation energy with the available experimental data shows a very good agreement for the lowest $np\sigma_u\ ^3\Pi_u$ state, but a ten percent discrepancy is found for the $3s\sigma_g\ ^{1,3}\Pi_g$ states. The ionization energies are found to be insenstive to the O_2^+ core wave functions. Variation of the ionization energies with the internuclear distance R is generally a few percent or less from R = 1.0 to 1.4$\AA$.

Next we study the O_2 Rydberg states that converge to the excited states of the parent O_2^+ ion, i.e., the $B^2\Sigma_g^-, b^4\Sigma_g^-$, and $c^4\Sigma_u^-$ states of O_2^+. The wave functions of the Rydberg electron are again determined by a Hartree-Fock scheme. The calculations cover $(n\ell)$ from (3.0) to (10,7) with m=0 and 1. For the internuclear distance we choose the equilibrium distances of the parent excited O_2^+ states and also R = 1.2$\AA$. The results are compared with photoabsorption and electron-impact energy-loss experiments. Good agreement is seen for the $ns\sigma_g$ $np\sigma_u$, and $np\pi_u$ series but the $nd\sigma_g$ states show larger discrepancy.

Details of our works have been published in

(a) Journal of Physics B: Atomic, Molecular and Optical Physics,
Volume 21, pp. 1155-1165 (1988),

(b) Physical Review A, Volume 39, pp.2367-2373 (1989).

PART 4

ELECTRON-IMPACT EXCITATION CROSS SECTIONS OF THE RYDBERG OXYGEN MOLECULES

We have formulated a scheme for calculating electron-impact excitation cross sections for the Rydberg states of the oxygen molecule by means of the method of close coupling. This was based on our earlier works on the application of the method of close coupling to calculate cross sections for electron-impact excitation of electronic states of the H_2 and N_2 molecules. In the earlier works we were dealing with excitation into the low-lying electronic states of N_2 and H_2, the wave functions of which were expressed as linear combinations of atomic-like orbitals at each nucleus, i.e., in the two-center form. In the present work we consider excitation into the Rydberg states of O_2, and their wave functions are expressed in the one-center form. A considerable modification had to be made in order to adapt the final-state wave functions to the one-center form. We have used this method of close coupling to calculate the cross sections for exciting O_2 from the ground electronic state ($X^3\Sigma_g^-$) to the $[O_2^+(b^4\Sigma_u^-)](3p\sigma_u)^3\Sigma_u$ Rydberg state at 60 and 80 eV and the results agree with those of the Born approximation to within 4%. This indicates that the Born approximation is sufficiently accurate for this work.

We have made a comprehensive study of electron-impact cross sections for exciting the oxygen molecule from the ground electronic state to the $ns\sigma_g$, $np\sigma_u$, $nd\sigma_g$, $nf\sigma_u$, $np\pi_u$, $nd\pi_g$, and $nf\pi_u$ Rydberg states associated with the $O_2^+(B^2\Sigma_g^-)$ and $O_2^+(b^4\Sigma_g^-)$ cores. The cross sections are calculated by the Born-Ochkur and Born-Rudge approximations. The wave function of the $X^3\Sigma_g^-$ ground state of O_2 is determined by a multiconfiguration self-consistent-field calculation. For each Rydberg orbital associated with the $O_2^+(B^2\Sigma_g^-)$ core, we have a singlet and a triplet state, whereas each Rydberg orbital associated with the $O_2^+(b^4\Sigma_g^-)$ core gives rise to a triplet and a quintet state. Since the ground sate of the O_2 molecule is a triplet, we have both spin-conserving and spin-changing excitation. At high

energies the excitation function for the spin-conserving excitation are found to conform to the Bethe-type asymptotic forms, whereras the excitation functions for the spin-changing excitation show the characteristic E^{-3}-dependence at large E. Once the cross sections are available up to 200 eV, one can easily extrapolate to higher energies.

Within each Rydberg series of a given ℓ, m, and O_2^+ core state, the shape of the excitation function is nearly identical for the various n-member except the first member (the lowest level) for which the excitation function has a somewhat different shape with the peak at a slightly lower energy. Furthermore, for each series, cross sections of the various n-members (except the first member) exhibit an n dependence of the form $n^{-\alpha}$ with α varying from one series to another in the range of 1.47 to 4.60 in contrast to the more universal n^{-3} dependence for the hydrogen atom.

Details of this work have been published in the Physical Review A, Volume 42, pp. 4391-4394 (1990).

PART 5

EMISSION CROSS SECTIONS FOR THE SECOND NEGATIVE BAND SYSTEM OF OXYGEN PRODUCED BY ELECTRON IMPACT

We have measured the absolute optical emission cross sections for the $O_2^+(A^2\Pi_u, v' \rightarrow X^2\Pi_g, v'')$ second negative band system for v' from 0 to 13 produced by electron impact with O_2 in the ground state $(X^3\Sigma_g^-, v = o)$ for incident electron energy from 0 to 500 eV. A monoenergetic, narrow electron beam of current about $90\mu A$ is passed through a collision chamber filled with oxygen gas at a presure about 10 mTorr. By measuring the absolute intensity of the emission for the various $v' \rightarrow v''$ bands, we have determined the absolute optical emission cross sections for some 28 bands. There are a number of emission bands that are too weak to be detected in an electron-beam experiment. For some of these weak bands, we used an indirect method to obtain the emission cross sections. In an oxygen-gas discharge the second negative emission bands are much stronger, but the $O_2^+(A^2\Pi_u, v')$ levels are populated by mechanisms that are more complicated than direct electron excitation. However, regardless of the mechanisms of population, the ratio of the intensity of two bands originating from the same upper state is equal to the ratio of the corresponding optical emission cross sections, i.e.,

$$\frac{I\left(v' \rightarrow v_j''\right)}{I\left(v' \rightarrow v_k''\right)} = \frac{Q^{opt}\left(v' \rightarrow v_j''\right)}{Q^{opt}\left(v' \rightarrow v_k''\right)} \tag{54}$$

Suppose we have measured the emission cross section of a strong band, $v' \rightarrow v_k''$, but the $v' \rightarrow v_j''$ band is too weak to detect in an electron-beam experiment. Thus we resort to an oxygen discharge in which all the bands are much stronger, to determine the intensity ratio $[I(v' \rightarrow v_j'')/I(v' \rightarrow v_k'')]$. Combining this intensity ratio with the measured cross section $Q^{opt}(v' \rightarrow v_k'')$, we can then obtain the cross section for the weaker band $v' \rightarrow v_j''$. In this manner we have obtained the emission cross sections for a number of weaker bands. From these optical emission cross section data we determine the apparent cross sections for ionization-excitation to 14 vibrational levels of $O_2^+(A^2\Pi_u, v')$ are determined.

We have measured the variation of emission radition intensity of the $5 \rightarrow 4$ band of the Second Negative System with the radial distance from the center of the electron beam. The result is shown in Figure 15. There is no significant tailing of the intensity with increasing distance. Therefore, this measurement does not show evidence of a significant long-life component in the population.

Details of our study of the cross sections for the second negative band system have been published in Physical Review A, Volume 38, pp.4537-4545 (1988).

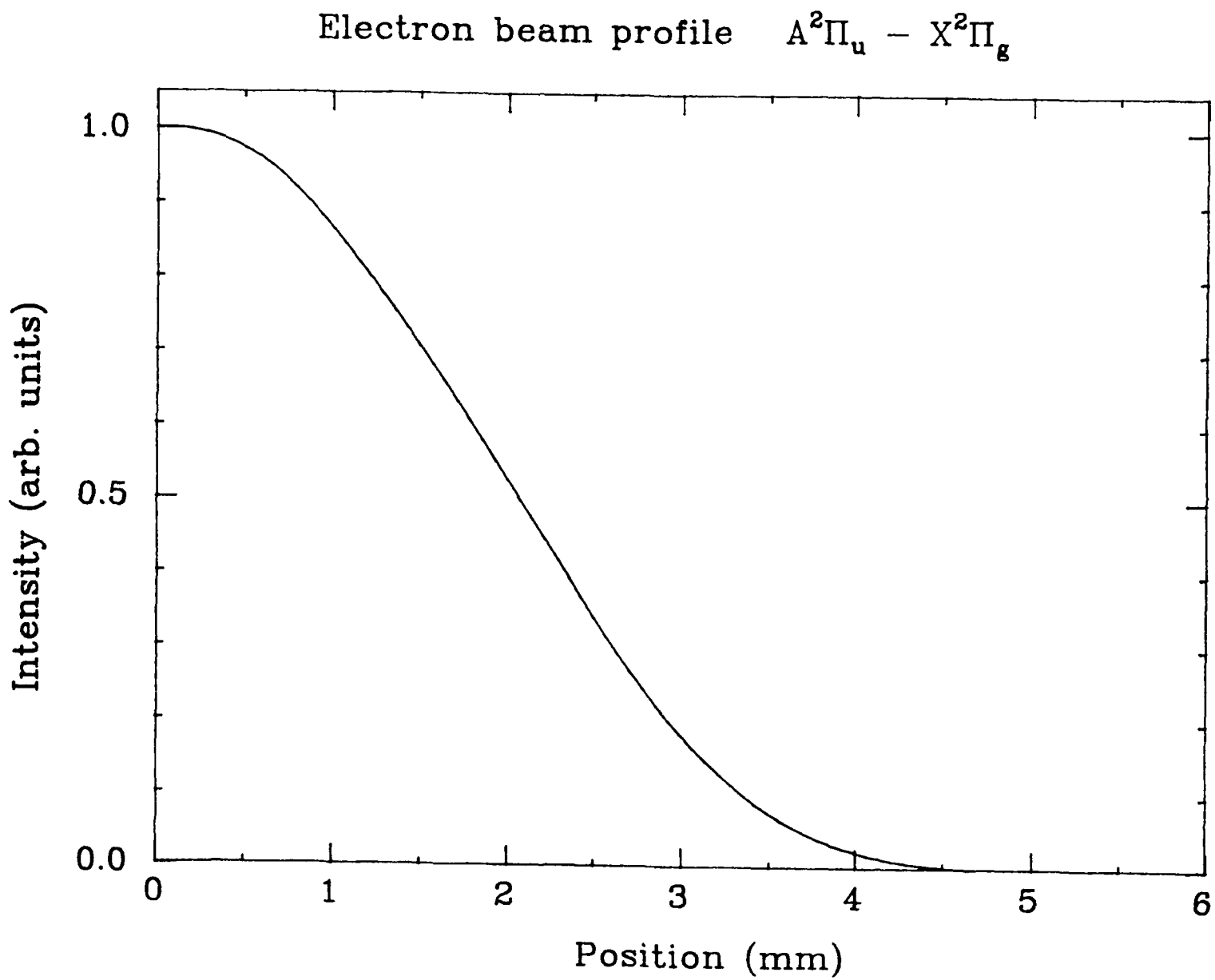

Figure 15. Variation of the emission radiation intensity of the 5-4 band of the Second Negative System of the oxygen molecule with the radial distance from the center of the electron beam.

PART 6

FORMATION OF HIGHLY EXCITED STATES BY ELECTRON RECOMBINATION WITH ATOMIC AND MOLECULAR OXYGEN IONS

Cross sections for radiative recombination of electrons with ground-state oxygen ions to form oxygen atoms in the $O[(^4S)n\ell]^{3,5}L$ states have been calculated for $n\ell$ up to (15,14) at 19 electron energies from 0.0345 to 2.585 eV. The wave functions for the bound states and the continuum states are determined by the Hartree-Fock method. Extrapolation of the cross sections to n>15 enables us to determine the radiative recombination rate coefficients at different temperatures. Analysis of the individual cross sections show that our calculated cross sections are very close to those obtained by using the hydrogenic approximation for $\ell \geq 2$. This is because the centrifugal barrier keeps the active electron from sampling the bound electrons of O^+, so that only the net positive charge of the O^+ ion is important. Therefore, the cross sections that we have obtained for electron radiative recombination with O^+ to form oxygen atoms in the $n\ell$ states with $\ell \geq 2$ are also applicable to radiative recombination of electrons with O_2^+ to form the corresponding $n\ell$ Ryderg states of the O_2 molecule. More details of this work can be found in our paper which was published in Physical Review A, Volume 43, pp.3433-3439 (1991).

PUBLICATIONS

1. S. Chung, C. C. Lin, and E. T. P. Lee "Electronic Structure of Rydberg Levels of the Oxygen Molecule", J. Phys. B **21** 1155 (1988).

2. R. S. Schappe, M. B. Schulman, F. A. Sharpton, and C. C. Lin "Emission of the $O_2^+(A^2\Pi_u \rightarrow X^2\Pi_g)$ Second-Negative-Band System produced by Electron Impact on O_2", Phys. Rev. A **38**, 4537 (1988).

3. S. Chung, C. C. Lin, and E. T. P. Lee "Rydberg Levels of the Oxygen Molecule Associated with Excited States of the Ion Core", Phys. Rev. **39**, 2367 (1989).

4. S. Chung, C. C. Lin, and E. T. P. Lee "Electron-Impact Excitation of the Rydberg Levels of the Oxygen Molecule", Phys. Rev. A **42**, 4391 (1990).

5. S. Chung, C. C. Lin, and E. T. P. Lee "Radiative-Recombination Cross Sections and Rate Coefficients of Atomic Oxygen", Phys. Rev. A **43**, 3433 (1991).

6. S. Chung, C. C. Lin, and E. T. P. Lee "Electron-Impact Ionization of the Oxygen Atom", submitted to Phys. Rev. A for publication.